



## Unravelling Heterogeneities in Complement and Antibody Opsonization of Individual Liposomes as a Function of Surface Architecture

Münter, Rasmus; Stavnsbjerg, Camilla; Christensen, Esben; Thomsen, Mikkel E.; Stensballe, Allan; Hansen, Anders E.; Parhamifar, Ladan; Kristensen, Kasper; Simonsen, Jens B.; Larsen, Jannik B.

Total number of authors:

11

Published in:

Small

Link to article, DOI:

[10.1002/smll.202106529](https://doi.org/10.1002/smll.202106529)

Publication date:

2022

Document Version

Peer reviewed version

[Link back to DTU Orbit](#)

Citation (APA):

Münter, R., Stavnsbjerg, C., Christensen, E., Thomsen, M. E., Stensballe, A., Hansen, A. E., Parhamifar, L., Kristensen, K., Simonsen, J. B., Larsen, J. B., & Andresen, T. L. (2022). Unravelling Heterogeneities in Complement and Antibody Opsonization of Individual Liposomes as a Function of Surface Architecture. *Small*, 18(14), Article 2106529. <https://doi.org/10.1002/smll.202106529>

---

### General rights

Copyright and moral rights for the publications made accessible in the public portal are retained by the authors and/or other copyright owners and it is a condition of accessing publications that users recognise and abide by the legal requirements associated with these rights.

- Users may download and print one copy of any publication from the public portal for the purpose of private study or research.
- You may not further distribute the material or use it for any profit-making activity or commercial gain
- You may freely distribute the URL identifying the publication in the public portal

If you believe that this document breaches copyright please contact us providing details, and we will remove access to the work immediately and investigate your claim.

**Unravelling heterogeneities in complement and antibody opsonization of individual liposomes as a function of surface architecture**

*Rasmus Münter, Camilla Stavnsbjerg, Esben Christensen, Mikkel E. Thomsen, Allan Stensballe, Anders E. Hansen, Ladan Parhamifar, Kasper Kristensen, Jens B. Simonsen, Jannik B. Larsen\*, Thomas L. Andresen\**

R. Münter, C. Stavnsbjerg, E. Christensen, A. E. Hansen, L. Parhamifar, K. Kristensen, J. B. Simonsen, J. B. Larsen, T. L. Andresen  
Biotherapeutic Engineering and Drug Targeting  
Department of Health Technology  
Technical University of Denmark (DTU)  
2800 Kgs. Lyngby  
Denmark

E-mail: [jannla@dtu.dk](mailto:jannla@dtu.dk), [tlan@dtu.dk](mailto:tlan@dtu.dk)

M. E. Thomsen, A. Stensballe  
Department of Health Science and Technology  
Aalborg University  
9220 Aalborg Ø  
Denmark

Keywords: opsonization, complement, accelerated blood clearance, heterogeneity, single liposome imaging

Coating nanoparticles with poly(ethylene glycol) (PEG) is widely used to achieve long-circulating properties after infusion. While PEG reduces binding of opsonins to the particle surface, immunogenic anti-PEG side-effects show that PEGylated nanoparticles are not truly “stealth” to surface active proteins. A major obstacle for understanding the complex interplay between opsonins and nanoparticles is the averaging effects of the bulk assays that are typically applied to study protein adsorption to nanoparticles. Here, we present a novel microscopy-based method for directly quantifying opsonization at the single nanoparticle level. We investigate various surface coatings on liposomes, including PEG, and show that opsonization by both antibodies and complement C3b is highly dependent on the surface chemistry. We further demonstrate that this opsonization is heterogeneous, with opsonized and non-opsonized liposomes co-existing in the same ensemble. Surface coatings modify the percentage of opsonized liposomes and/or opsonin surface density on the liposomes, with strikingly different

patterns for antibodies and complement. Thus, this assay provides mechanistic details about opsonization at the single nanoparticle level previously inaccessible to established bulk assays.

## 1. Introduction

When nanoparticles are exposed to a biological environment such as blood, their surfaces adsorb opsonins, which are proteins of the immune system destining the particle for removal by the body's natural clearing machinery.<sup>[1,2]</sup> The most common method for reducing opsonization of nanoparticles is by surface-coating them with polyethylene glycol (PEG), which has been essential for bringing especially liposomal drugs into the clinic.<sup>[3–5]</sup> Initial evidence supported that PEGylation reduced opsonization of the liposomal surfaces by creating a steric barrier.<sup>[6]</sup> However, the complexity of this concept is apparent from studies showing that complement C3 and antibodies efficiently bind PEGylated liposomes,<sup>[7,8]</sup> hamper the performance of liposomal systems,<sup>[9]</sup> and in the most extreme cases induce hypersensitivity reactions<sup>[10,11]</sup> or accelerated clearance upon repeated injections.<sup>[12,13]</sup> Thus, the current ambiguity regarding the immunological requirements for *stealth* properties<sup>[14]</sup> – reduced opsonization<sup>[15]</sup> or increased dysopsonization<sup>[16]</sup> – represents a bottleneck for overcoming the widely recognized translational gap in nanomedicine.<sup>[17–19]</sup>

Traditionally, anti-liposome antibodies are studied by ELISA.<sup>[20–23]</sup> ELISAs are however claimed to suffer from non-specific binding and – since individual PEG-moieties are simply adsorbed to a flat surface – does not reflect binding to authentic liposomal surfaces with respect to PEG density and topology, lipid mixture, surface curvature, as well as membrane-charge and –fluidity.<sup>[24–26]</sup> Alternatively, liposome opsonization has been studied using bulk biochemical assays, where the protocol includes crude centrifugation steps and/or extensive washing procedures, before opsonization is inferred from indirect detection methods.<sup>[7,24,25,27]</sup> The validity of such separation-based approaches has been questioned due to concerns about contamination of non-bound proteins in the nanoparticle isolates.<sup>[28–31]</sup> In addition, such bulk

assays report only average ensemble values, thereby intrinsically assuming all liposomes in the sample to be identical.<sup>[32,33]</sup> However, it is increasingly recognized that opsonization might be heterogeneous between nanoparticles and that this variation could have great functional importance,<sup>[1,31,33,34]</sup> prompting the need for new and more sophisticated assays.<sup>[24,25,35]</sup> Investigating opsonization heterogeneity however means studying individual liposomes in complex biological environments, which is a formidable task due to their nanoscale size. Imaging methodologies capable of directly detecting protein adsorption to individual particles, have only very recently emerged.<sup>[34,36,37]</sup> Unfortunately, the translational impact of these studies is limited as they rely on modified proteins and extensive sample preparations (including washing, centrifugation and fixation). Detailed understanding of the opsonization of individual liposomes is hence still lacking. Gaining such understanding is however of utmost importance, considering the extensive clinical use<sup>[38]</sup> and hampering clinical challenges<sup>[10,11,39,40]</sup> of liposomes.

Here, we develop and employ a novel microscopy-based single-particle assay for studying the association of two major types of opsonins – antibodies (IgG and IgM) and complement C3b – directly to individual liposomes modified with various surface coatings. This Single Liposome Opsonization Measurement (SLOM) assay permits for precisely distinguishing actual liposome-association from non-specific background with a previously unseen sensitivity in complex biological environments, such as complete human plasma or plasma from mice pre-treated with similar liposomes. SLOM allowed us to reveal the co-existence of opsonized and non-opsonized liposomes in the same ensemble and to quantify the opsonin surface density on individual liposomes. We used SLOM to demonstrate how liposomal surface decorations (including PEG and drugs) promote opsonization by IgM, IgG and complement C3b. Increased opsonization materialized as either increased percentage of opsonin-positive liposomes or increased opsonin surface density, with different mechanistic patterns for the proteins studied. Our methodology allows for detailed studies on the molecular, compositional and

physicochemical features governing liposome opsonization with single particle resolution. Beyond expanding the fundamental knowledge on protein adsorption to liposomes, we envision that the ability to study in detail the immunogenicity of all liposomal formulation and even detect if only a subpopulation of the liposomes drives the immunogenicity, will be essential for developing next generation nanomedicines and allow to screen for designs that avoid the immunogenic challenges associated with nanoparticles in a clinical setting.

## 2. Results and Discussion

### 2.1. Opsonized and non-opsonized liposomes co-exist in the ensemble

To study opsonin association to individual liposomes we developed and employed the SLOM assay. Briefly, we immobilised fluorescently labelled (DiD) liposomes on a passivated glass surface as previously described<sup>[41–44]</sup> and incubated them in plasma (**Figure 1a**). After incubation, we removed the plasma, added AF488-labelled detection antibodies against the opsonin of interest, and employed confocal microscopy to image the DiD and AF488 channels (**Figure S1-S3**, Supporting Information). Opsonized liposomes were identified based on spatial co-localisation between the DiD and AF488 fluorescence, allowing us to elucidate three different scenarios: a fraction of liposomes displaying no detectable opsonization (I, **Figure 1b**), opsonins not interacting with liposomes (II, **Figure 1b**) and a fraction of liposomes displaying strong opsonization (III, **Figure 1b**). The high-throughput nature of the SLOM assay allowed sampling of hundreds of liposomes per image frame and quantifying the frequency of all three scenarios using automated image analysis. The microscopy-based approach circumvented the need for washing with detergents (a drawback for many anti-PEG ELISAs<sup>[26]</sup>) since the analysis enabled filtering out non-specific binding opsonin signal (II, **Figure 1b**) allowing us to investigate only true binding events (III, **Figure 1b**).

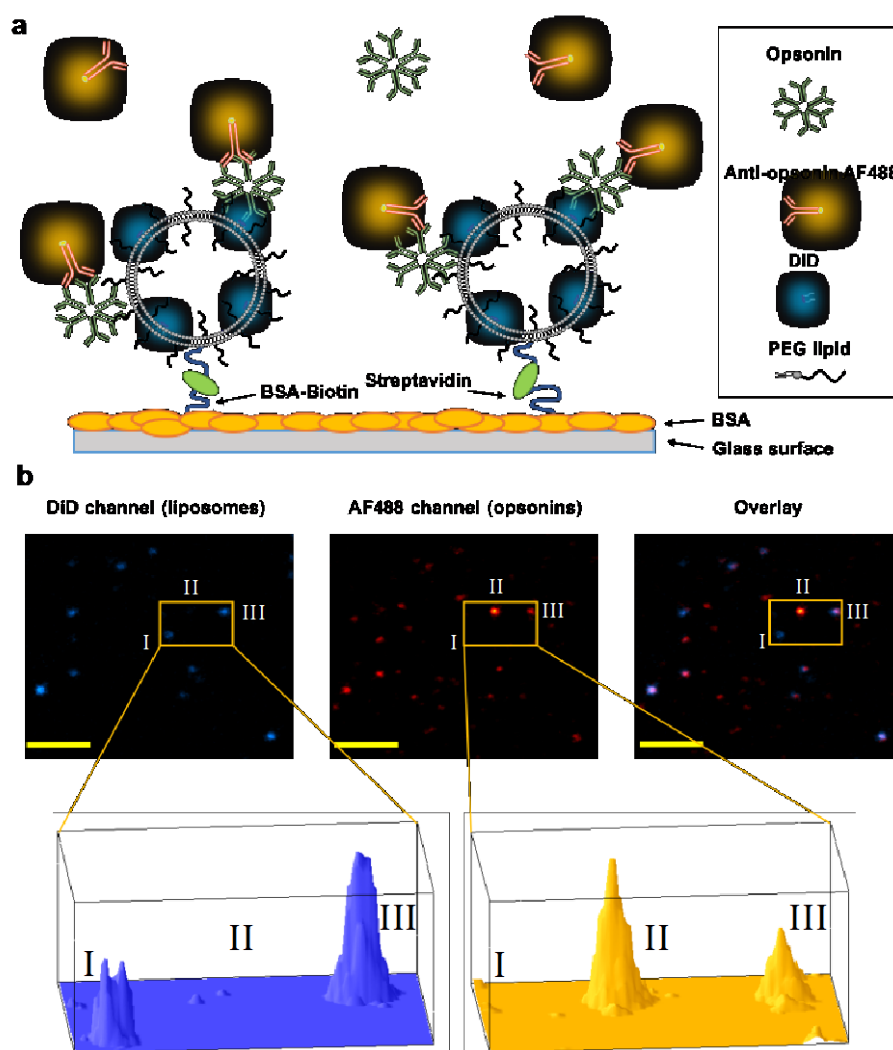


**Figure 1.** Single Liposome Opsonization Measurement (SLOM) setup

a) Fluorescently labelled (DiD) liposomes are immobilised on passivated surfaces with a biotin/streptavidin linker, incubated with plasma, and association of a specific opsonin (e.g. IgM) is measured with fluorescently labelled (e.g. AF488) primary antibodies, b) Micrographs of the DiD channel (liposomes) (left) and the AF488 channel (opsonin) (right), evaluating the spatial co-localization of signal in the two channels reveal three potential scenarios: I) Liposome with no detectable opsonin association, II) Opsonin adsorbed to the BSA surface, not co-localized with any liposome and hence not included in the downstream analysis, III) Liposome with associated opsonin. Scale bars are 2.5  $\mu\text{m}$ .

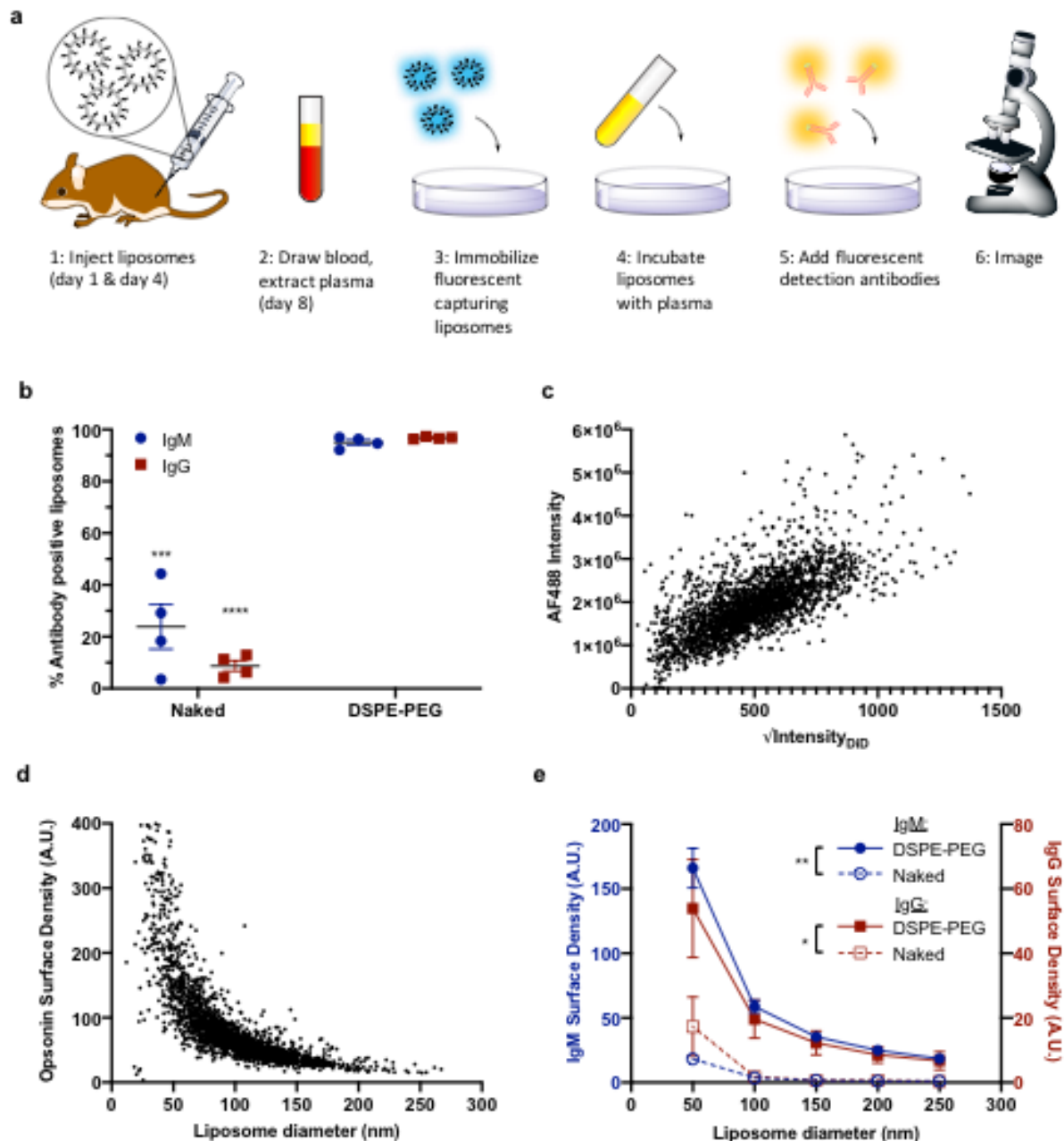


**Figure 2.** PEGylation and liposome size regulates antibody opsonization of individual liposomes.

The figure shows antibody (IgM and IgG) association to DSPE-PEG or Naked liposomes in mouse plasma investigated using the SLOM assay. a) Assay procedure for quantifying anti-PEG antibodies in mouse plasma. b) The percentage of IgM (blue) and IgG (red) positive liposomes out of a total ensemble of approx. 3000 liposomes per sample. Error bars show SEM of variation between individual animals,  $n = 4$  c) Square root of the DiD intensity ( $\sqrt{\text{Intensity}_{\text{DiD}}}$ ) of each individual liposome plotted against the AF488 intensities of the corresponding liposome

in a representative experiment studying binding of IgM to DSPE-PEG liposomes. d) The intensity data for each individual liposome in b converted to opsonin surface density versus liposome diameter in nm. e) Mean IgM (blue) and IgG (red) surface density on DSPE-PEG liposomes (solid lines, filled circles) and Naked liposomes (dashed lines, open circles) for various liposome size groups. Error bars show SEM of variation between individual animals,  $n = 4$ . ~~fe) The percentage of C3b positive liposomes out of a total ensemble of approx. 3000 liposomes per sample,  $n = 5$  for DSPE-PEG (light blue) and  $n = 6$  for Naked (open circles). Error bars show SEM of variation between donors. gf) C3b surface density on DSPE-PEG (light blue) and Naked (open circles) liposomes for various liposome size groups. Error bars show SEM of variation between donors,  $n = 5$  for DSPE-PEG and  $n = 6$  for Naked. Antibody association was measured in plasma from mice pre-treated with intravenous injections of corresponding liposomes., C3b association was detected in human plasma from non-treated healthy donors. Statistics in b are based on a two-tailed unpaired t-test, comparing association to Naked and DSPE-PEG liposomes for the specific opsonin class. Statistics in d are based on a two-way ANOVA with Tukey's correction for multiple comparisons. \* $p < 0.05$ , \*\* $p < 0.005$ , \*\*\* $p < 0.0005$ , \*\*\*\* $p < 0.0001$ , N.S = not significant.~~

To determine how liposome PEGylation affected antibody-generation and –association to individual liposomes upon repeated exposure, we initially compared two liposomal systems: Naked (DSPC:Cholesterol 61.8:38.2 molar ratio) and DSPE-PEG (DSPC:Cholesterol:DSPE-PEG 56.6:38.2:5.2 molar ratio), (**Table S1**, Supporting Information). First, we pre-treated mice with two doses of either Naked or DSPE-PEG liposomes ( $0.1 \mu\text{mol phospholipid kg}^{-1}$ ) with a four-day interval and drew blood on day eight; a dosing schedule commonly used to study generation of anti-PEG antibodies.<sup>[12,13]</sup> Antibody association (both IgM and IgG) to corresponding Naked and DSPE-PEG liposomes was analysed with the SLOM assay, by immobilizing either Naked or DSPE-PEG liposomes in microscopy wells, incubating these

liposomes with plasma from liposome-treated mice, incubating the liposomes with fluorescently labelled anti-mouse IgM or anti-mouse IgG antibodies and finally imaging the liposomes (**Figure 2a**). After incubation in plasma from mice treated with DSPE-PEG liposomes, we found that the average percentage of IgG and IgM positive liposomes in the ensemble ( $\%IgG^+$  and  $\%IgM^+$ ) was  $96.8 \pm 0.2 \%$  and  $95.0 \pm 1.0 \%$ , respectively (**Figure 2b**). When incubating Naked liposomes in plasma from mice treated with Naked liposomes, the  $\%IgM^+$  value varied from 4.0 % to 44 %, whereas  $\%IgG^+$  was consistently below 10% (**Figure 2b**). The existence of a liposome population not displaying detectable opsonization is not a mere artefact of our detection limit excluding identification of low-level opsonization of small liposomes, as this behaviour was seen for all liposome sizes (**Figure S4**, Supporting Information). These data show for the first time, under minimally invasive native-like conditions, that antibody association is heterogeneous between individual liposomes, with a fraction of liposomes being antibody-positive and another being antibody-negative. The fraction of antibody-positive liposomes was significantly increased by liposome PEGylation, demonstrating that PEGylation increases antibody-generation.

Liposome size has previously been claimed to affect the opsonization of liposomes.<sup>[31,45]</sup> Nevertheless, traditional bulk assays cannot accurately correct for the intrinsic size heterogeneity present even for liposomes homogenised by extrusion,<sup>[43,46]</sup> and are thus limited to intrinsically assume all liposomes in an extruded batch to have the same size. Here, to more accurately investigate the size-dependency of opsonization, we extracted the DiD and AF488 intensities of the individual liposomes (**Figure 2c**), and converted DiD intensity to liposome diameter by combining microscopy and Dynamic Light Scattering as previously described (**Figure S5**, Supporting Information).<sup>[46–48]</sup> Next, we calculated the opsonin surface density on each individual liposome as the ratio between its integrated AF488 and DiD intensities (**Figure 2d**). To compare the antibody density between different liposome formulations we plotted the

antibody density versus liposome size pooled into 50 nm size intervals (Figure 2d). For antibody association to the DSPE-PEG liposomes, this analysis revealed a clear liposome-size dependency on the average IgG and IgM densities. Association to DSPE-PEG liposomes in the 50 nm bins was hence  $9.0 \pm 0.2$  fold higher than in the 250 nm bins for IgM and  $9.2 \pm 1.1$  fold higher for IgG (Figure 2e). This indicates that liposome size might be a strong regulator of antibody association, with increasing membrane curvature leading to significantly higher antibody surface-densities. Such size-dependencies of protein binding to nanoparticles has often been discussed<sup>[12,45]</sup> and while the underlying mechanism remains unresolved, it could be matter of imperfect lipid packing or curvature dependent differences in the arrangement of PEG chains on the liposome surface.<sup>[49,50]</sup> Importantly, this size dependency would not only have been hidden in traditional bulk assays, but the presence of 50 nm liposomes in a liposome batch that (e.g. after extrusion through a 200 nm pore-size filter) is assumed to have a size of 200 nm could skew the mean value that would be the output result of such assays.

To elucidate how PEGylation affected the amount of antibodies associated to liposomes, we compared the average antibody surface densities on Naked and DSPE-PEG liposomes. Doing this, we found higher association to DSPE-PEG versus Naked liposomes for both IgG and IgM across all size-groups ( $10.6 \pm 2.2$  fold higher for IgG and  $17.2 \pm 2.0$  fold higher for IgM for the most populous 100 nm size-group) (Figure 2e). It should be emphasized that the data cannot confirm if the antibodies bind directly to the PEG chains on the liposomal surface, or indirectly through other adsorbed plasma proteins. Additional experiments revealed that there were no detectable anti-PEG antibodies in plasma from mice not previously exposed to liposomes (**Figure S6**, Supporting Information). Further, antibody-recognition of the liposomes was dependent on the presence of PEG, as there was very little association when Naked liposomes were incubated in plasma from mice treated with DSPE-PEG liposomes (**Figure S7**, Supporting Information). In agreement with earlier findings<sup>[51]</sup> we therefore concluded that exposure to

PEGylated liposomes results in high amounts of antibodies able to recognise PEGylated liposomes, whereas very low amounts of anti-liposome antibodies are generated in response to treatment with Naked liposomes.

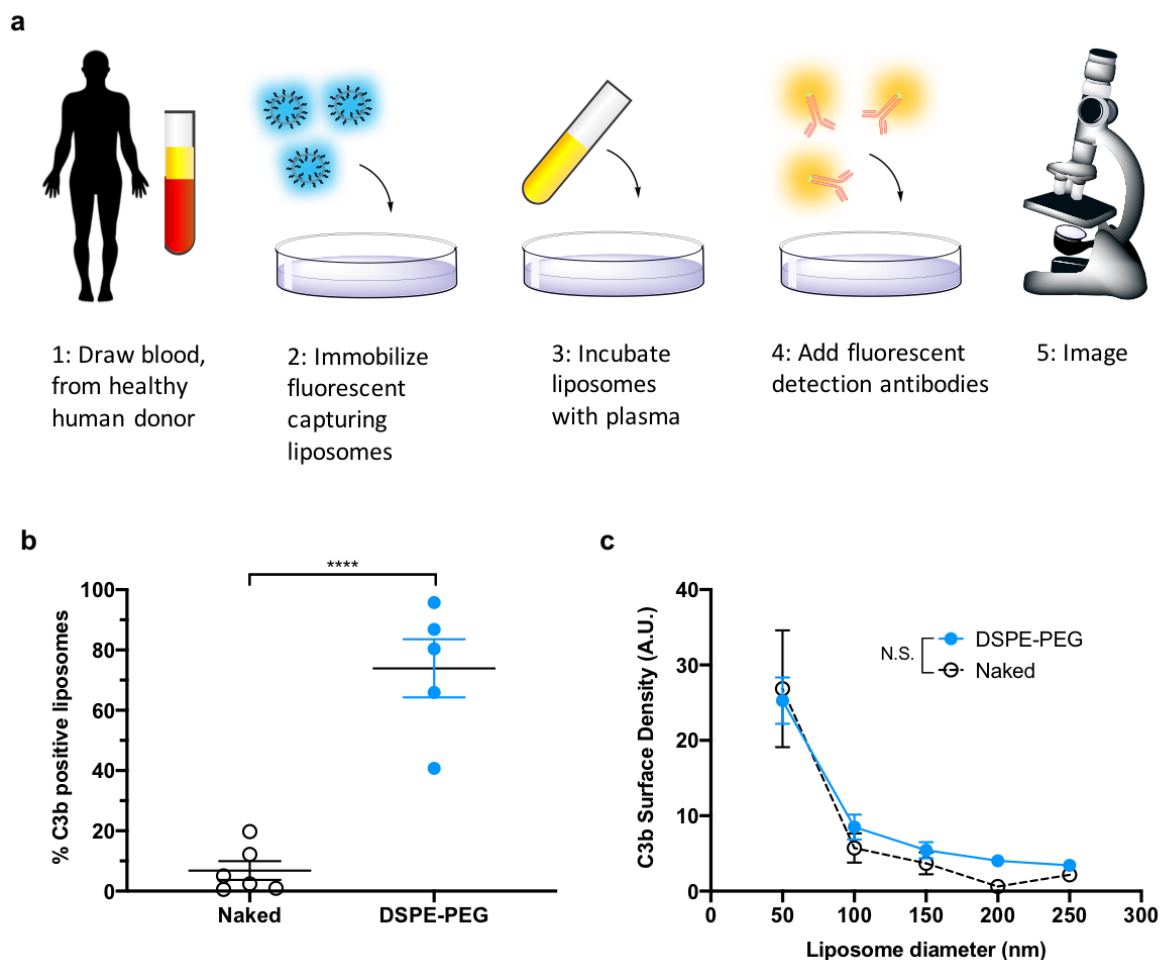


**Figure 3.** PEGylation and liposome size regulates complement opsonization of individual liposomes.

The figure shows complement (C3b) association to DSPE-PEG or Naked liposomes in human plasma investigated using the SLOM assay. a) Assay procedure for quantifying anti-PEG antibodies in human plasma. b) The percentage of C3b positive liposomes out of a total ensemble of approx. 3000 liposomes per sample,  $n = 5$  for DSPE-PEG (light blue) and  $n = 6$  for Naked (open circles). Error bars show SEM of variation between donors. g) C3b surface density on DSPE-PEG (light blue) and Naked (open circles) liposomes for various liposome size groups. Error bars show SEM of variation between donors,  $n = 5$  for DSPE-PEG and  $n =$

6 for Naked. C3b association was detected in human plasma from non-treated healthy donors. Statistics are based on a two-tailed unpaired t-test, comparing association to Naked and DSPE-PEG liposomes b, and on a two-way ANOVA with Tukey's correction for multiple comparisons for c. \* $p < 0.05$ , \*\* $p < 0.005$ , \*\*\* $p < 0.0005$ , \*\*\*\* $p < 0.0001$ , N.S = not significant.

The complement system represent one of the most essential opsonization machineries, implicated both in the innate part of the immune system (and hence clearance in individuals not previously exposed to liposomes) as well as in adaptive immunity, potentially causing hypersensitivity reactions and drug leakage from liposomes.<sup>[10,11,26,40]</sup> Without the need of pre-exposure to liposomes, it was possible to study complement opsonization in blood plasma from healthy human donors instead of in mouse plasma (**Figure 3a**). To test if PEGylation affected the association of C3b (the central opsonin of complement<sup>[52]</sup>) to individual liposomes, we incubated immobilised Naked or DSPE-PEG liposomes with human plasma and investigated C3b association with SLOM using a FITC-labelled anti-C3b detection antibody. We quantified the average percentage of C3b positive liposomes (%C3b<sup>+</sup>) for the Naked system to be  $6.8 \pm 3.1$  %, representing a very low number, comparable to random co-localisation (**Table S2**, Supporting Information). In contrast, the %C3b<sup>+</sup> was between 41 % and 96 % for DSPE-PEG liposomes (Figure 3b). As similar findings could be achieved using a different antibody-clone (**Figure S8**, Supporting Information), and no association was observed in absence of plasma (**Figure S9**, Supporting Information), the data truly reflect C3b association and not unspecific adsorption of the detection antibody. Interestingly, C3b seems to bind indirectly to the liposomes through other adsorbed plasma proteins, as no association was observed when liposomes were incubated with pure C3 protein (**Figure S10**, Supporting Information).<sup>[8,53]</sup> The surface density of C3b also displayed a liposome size dependency, however the average C3b surface densities for Naked and DSPE-PEG liposome systems were generally similar (Figure 3c). It should be stressed that the number of C3b positive Naked liposomes is very low in some

donors, increasing the impact of potential false positives on the observed surface density (Table S2, Supporting Information). The overall increase in C3b association to PEGylated liposomes compared to Naked liposomes primarily due to the increased %C3b<sup>+</sup>, was corroborated by separation-based LC-MS/MS bulk measurements (**Figure S11 and S12**, Supporting Information) albeit without the ability to entangle the association percentage from the surface density. The high C3b-content in liposome-free plasma demonstrate another weakness of such crude separation-based assays, underlining the strength of our highly sensitive method in which C3b not associated to liposomes can easily be distinguished (**Figure S3**). Overall, for both antibodies and C3b, the single liposome analysis allowed us to describe the full opsonization landscape and delineate how PEGylation affected both the number of opsonin-positive liposomes and the opsonin surface density on these. This revealed fundamental differences in how PEGylation affected antibody and C3b opsonization. For antibodies, PEGylation increased both the number of positive liposomes and the surface density of opsonins, whereas PEGylation only increased the number of C3b positive liposomes, but not the C3b surface density. This represents a level of mechanistic detail previously inaccessible with the bulk methods employed to study liposome opsonization and underscores the importance of understanding opsonization at the single particle level.

## **2.2. Presentation of PEG on a liposomal surface is essential for proper IgM recognition**

Next, we investigated how the three-dimensional context of the PEG chain influences anti-PEG antibody opsonization. To study the importance of presenting the PEG-moiety in its native three-dimensional conformation on a liposomal surface, we performed a competition assay where plasma from mice previously receiving injections of DSPE-PEG liposomes was pre-incubated with either free PEG chains (mPEG2000), DSPE-PEG (forming micelles at concentrations >10 $\mu$ M<sup>[54]</sup>) or DSPE-PEG liposomes (**Figure 4a and 4b**). The solutions were then added to immobilised liposomes before the %IgM<sup>+</sup> value was quantified with SLOM. Thus,

a higher %IgM<sup>+</sup> value correlated to less initial anti-PEG IgM adsorption to the PEG compound during the pre-incubation. At comparable levels of 0.5  $\mu$ M total available PEG, the %IgM<sup>+</sup> value was reduced to  $21.2 \pm 4.0$  % for the DSPE-PEG liposome system, whereas both the free PEG and the DSPE-PEG micelle systems showed no significant reduction from the %IgM<sup>+</sup> value at 0  $\mu$ M PEG (Figure 4c). Competition from free PEG or DSPE-PEG micelles impacted the %IgM<sup>+</sup> values only for concentrations at or above 500  $\mu$ M (Figure 4c) and the surface density only at PEG concentrations higher than 5  $\mu$ M (Figure 4d). This demonstrates that IgM against DSPE-PEG liposomes has a much higher propensity to interact with PEG displayed on a liposomal surface than to PEG displayed in micelles or as free PEG. This highlights the limitations when employing non-liposomal anti-PEG antibody detection assays, as it is essential that PEG-moieties are displayed in the authentic three-dimensional orientation on liposomal surfaces for anti-PEG IgM to properly recognise it.

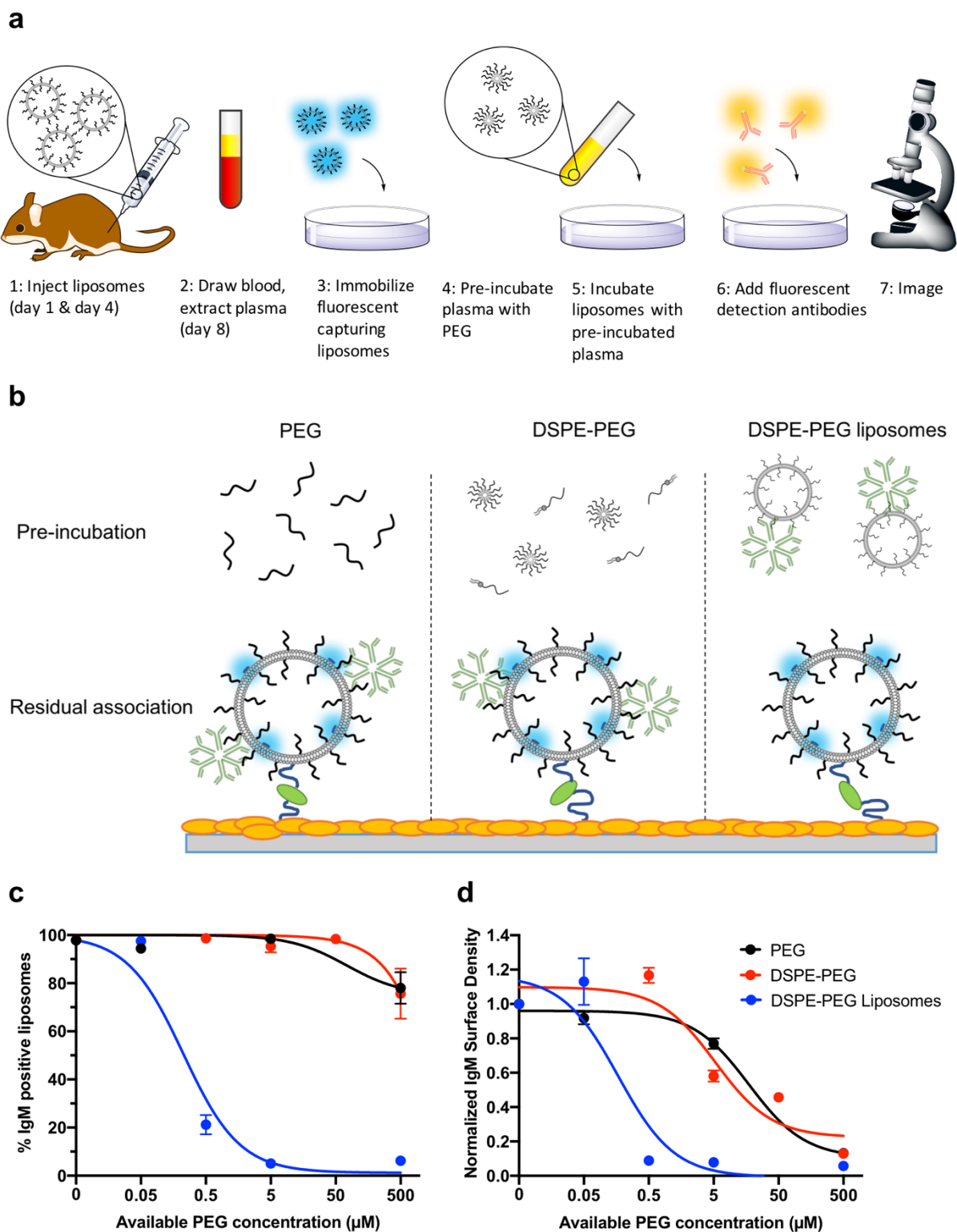


**Figure 4.** Anti-PEG IgM association strongly depends on the PEG chain being presented on a liposomal surface. a) Scheme showing the experimental procedure. b) Scheme of the competition assay where plasma is pre-incubated with free PEG, DSPE-PEG (as micelles at concentrations  $>10\mu\text{M}$ ) or DSPE-PEG liposomes before being added to the immobilized

liposomes. For liposomes, only half of the PEG was assumed to be presented on the outer leaflet of the membrane c) %IgM<sup>+</sup> as a function of available PEG concentration, d) IgM surface density normalized to the association without competition in the respective 50-nm size group, followed by averaging across the five size-groups. The relatively small error bars (showing SEM of the variation between the five size groups) hence indicate that the inhibition is similar in all size-groups, and that competition is independent of liposome size. Fits are a three-parameter dose-response inhibition functions. All plasma used in the experiment originated from the same mouse.

### **2.3. Promotion of opsonization is a prevalent phenomenon for liposomal surface decorations**

To investigate if antibody generation was specific for PEGylated liposomes or a general property for liposomal surface decorations, we formulated liposomes with the surface-displayed drug mifamurtide (DPPE-anchored muramyl tripeptide) – the active component in the clinically used liposome formulation Mepact.<sup>[55,56]</sup> In plasma from mice pre-treated with mifamurtide liposomes, we quantified very high %IgM<sup>+</sup> and %IgG<sup>+</sup> values as well as antibody surface densities (**Figure 5a-d (red)**), all at the level of the DSPE-PEG system or higher (**Figure S13, Table S4**, Supporting Information). Anti-mifamurtide antibodies were undetectable in plasma from treatment-naïve mice (**Figure S14**, Supporting Information). These results show that high amounts of specific antibodies were generated against the mifamurtide-coated liposomes. In human plasma, we also recorded a high %C3b<sup>+</sup> value for mifamurtide liposomes (**Figure 5e (red)**), comparable to the value for DSPE-PEG liposomes (**Table S5**, Supporting Information). The C3b surface density was higher for mifamurtide liposomes than for any other formulation in this study (**Figure 5f**). These data demonstrate that antibody generation and complement opsonization is not restricted to PEGylated surfaces, but is a more generic property that can also be facilitated by other liposomal surface decorations, including drugs.

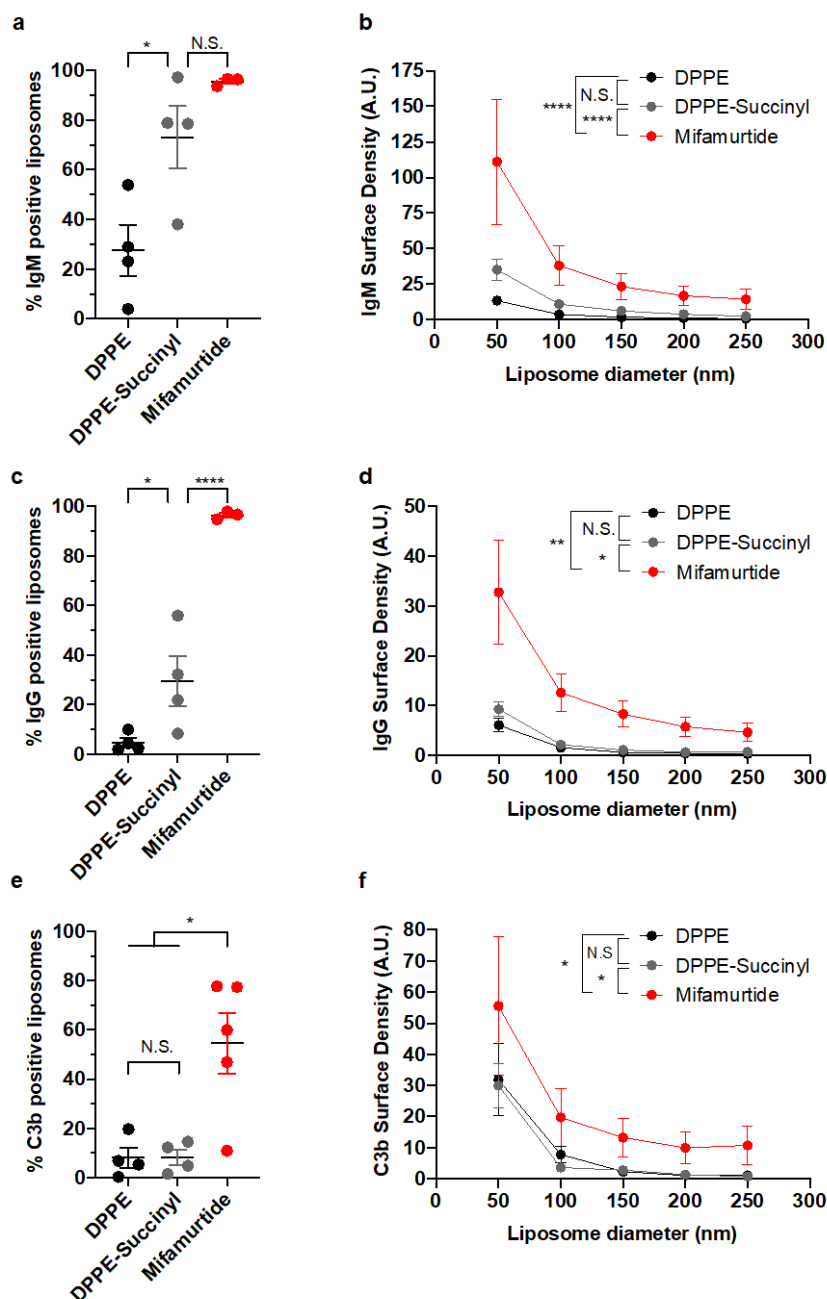


**Figure 5.** Lipid-conjugated drugs presented on liposomal surfaces can facilitate opsonization and antibody generation, suggesting this to be a generic property for liposomal surface decorations. a) Percentage of IgM positive liposomes. b) IgM surface density versus liposome diameter. c) Percentage of IgG positive liposomes. d) IgG surface density versus liposome diameter. e) Percentage of C3b positive liposomes. f) C3b surface density versus liposome diameter. In all graphs three liposome systems DPPE (black), DPPE-Succinyl (grey) and Mifamurtide (red) are compared with  $n = 3-5$ . IgM and IgG opsonisation was studied in mice

pre-treated with corresponding liposomes, C3b opsonisation was studied in blood plasma from non-treated healthy human donors. Each sample represent an ensemble of 2000-3000 individual liposomes. Error bars show SEM of donor variation. Statistics are based on a one-way (a, c, e) or two-way (b, d, f) ANOVA with Tukey's correction for multiple comparisons, \* $p < 0.05$ , \*\* $p < 0.005$ , \*\*\* $p < 0.0005$ , \*\*\*\* $p < 0.0001$ , N.S. = not significant.

We then set out to elucidate the molecular features facilitating opsonization of authentic liposomal surfaces at the single particle level, by systematically modifying the individual components of the lipid conjugates. First, to determine if the phosphoethanolamine (PE) lipid anchor or the phosphoamide linker, shared by both DSPE-PEG and mifamurtide (**Figure S15**, Supporting Information), induced opsonization of single liposomes, we formulated liposomes where the DSPE-PEG lipid was replaced by either DPPE or DPPE-Succinyl. We then measured antibody opsonization for these formulations in plasma from mice pre-treated with similar liposomes, and C3b opsonization in human plasma. For both antibody classes, we quantified lower percentages of positive liposomes for the DPPE system than for the DPPE-Succinyl system (Figure 5a and 5c). IgG and IgM surface densities were however similar on DPPE and DPPE-Succinyl liposomes across all liposome sizes (Figure 5b and 5d). No antibodies against the formulations were detected in mice not previously exposed to liposomes (Figure S8, Supporting Information). SLOM was hence able to reveal how the small phosphoamide-conjugated succinyl-group increased the association percentage of IgG and IgM without significantly altering the antibody surface-density. For C3b we only quantified minute %C3b<sup>+</sup> values for both DPPE and DPPE-Succinyl liposomes, comparable to what we observed for the Naked liposomes (Figure 5e, Table S5), indicating that these liposomes are only minimally opsonized by complement. This illustrates that neither the primary amine (able to interact with the reactive thioester of C3b<sup>[52]</sup>) on the PE anchor, the succinate on DPPE-Succinyl liposomes (suggested to mediate anti-PEG immunity<sup>[26]</sup>), nor the phosphate oxygen in phospholipid

conjugates (previously found to mediate complement activation by DSPE-PEG<sup>[57]</sup>) could facilitate noteworthy C3b association to liposomes. For the small amount of %C3b<sup>+</sup> liposomes, the average C3b surface density was similar for the DPPE and DPPE-Succinyl liposomes (Figure 5f). Overall, we found that modifying the various molecular features of lipid conjugates affected both the number of opsonin-positive liposomes and the opsonin density on the liposomes. Whereas the DPPE anchor in itself was not involved in opsonization, the small phosphoamide linker in DPPE-Succinyl resulted in increased antibody-generation. The strongest opsonization of both IgM, IgG and C3b was observed when the conjugate was a larger molecule such as a drug or a polymer.

Natural membrane systems, such as cells, avoid clearance by decorating their surface with so-called self-markers.<sup>[58,59]</sup> One such self-marker is GM1, a ganglioside, consisting of a sialic acid-containing oligosaccharide attached to a ceramide anchor (**Figure S16**, Supporting Information), which were previously demonstrated to impose *stealth* abilities to liposomes in mice.<sup>[60–62]</sup> To provide detailed mechanistic insights on how self-markers prolong liposome circulation, we tested if GM1 displayed on liposomal surfaces would also induce IgM, IgG or C3b opsonization. We formulated liposomes with GM1 and compared these to a PEG system also anchored by ceramide (Ceramide-PEG), by subjecting mice to repeated injections of such liposomes and measuring antibody-generation with SLOM. The %IgG<sup>+</sup> and %IgM<sup>+</sup> values were very low for the GM1 system – on the level of what we previously observed for Naked liposomes – but very high for the Ceramide-PEG system – on the level of the DSPE-PEG liposomes (**Figure 6a and 6c, Table S6**). We also recorded 9-17 fold higher IgM and 5-11 fold higher IgG densities on Ceramide-PEG versus GM1 liposomes across all sizes (Figure 6b and 6d). No antibodies against any of the constructs were observed in treatment-naïve mice (Figure S14, Supporting Information). Thus, the presence of the self-marker GM1 could effectively abolish the generation of anti-liposome antibodies.

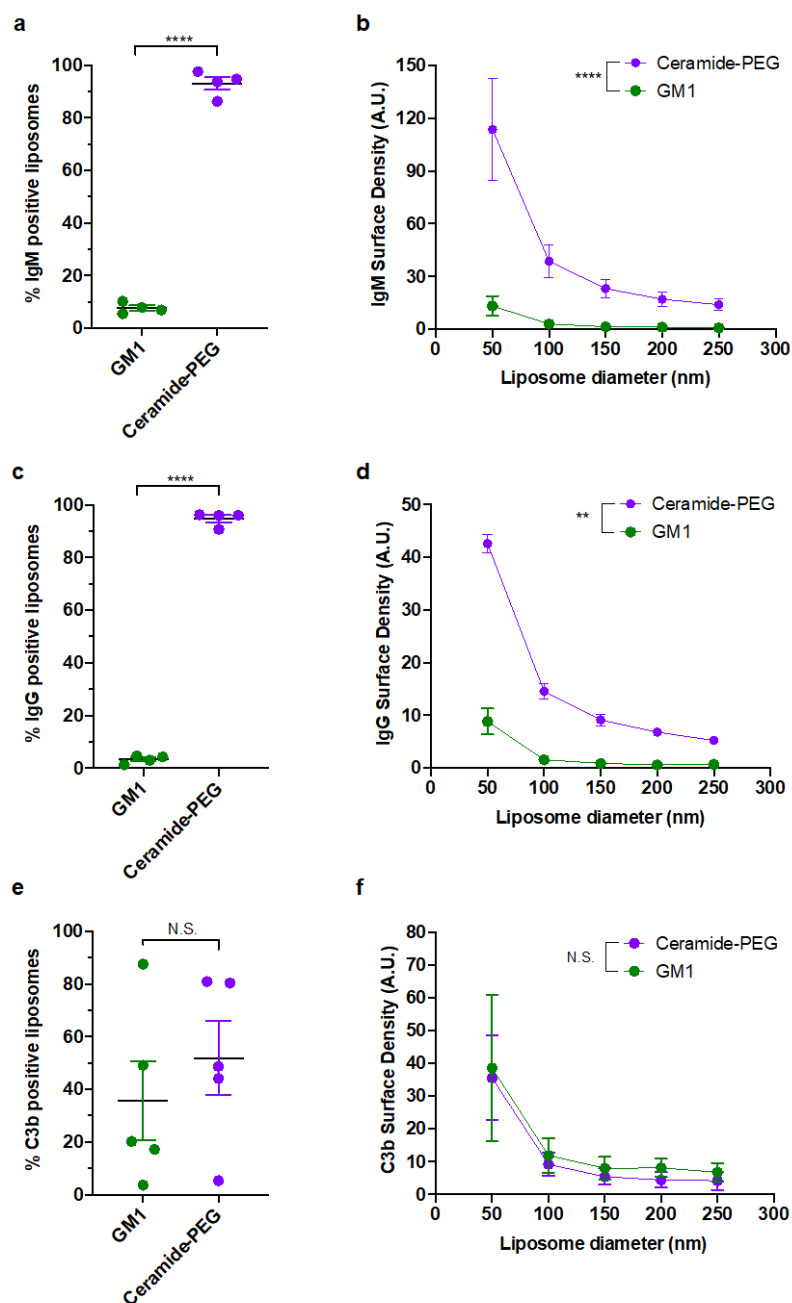


**Figure 6.** Self-markers on liposomes reduce antibody generation - steric barriers do not.

a) Percentage of IgM positive liposomes. b) IgM surface density versus liposome diameter. c) Percentage of IgG positive liposomes. d) IgG surface density versus liposome diameter. e) Percentage of C3b positive liposomes. f) C3b surface density versus liposome diameter. In all graphs two liposome systems GM1 (green) and Ceramide-PEG (purple) are compared and  $n = 4$  for IgM and IgG,  $n = 5$  for C3b. IgM and IgG opsonisation was studied in mice pre-treated with corresponding liposomes, C3b opsonisation was studied in blood plasma from non-treated

healthy human donors. Error bars show SEM of donor variation. Statistics are based on a one-way (a, c, e) or two-way (b, d, f) ANOVA with Tukey's correction for multiple comparisons, \* $p < 0.05$ , \*\* $p < 0.005$ , \*\*\* $p < 0.0005$ , \*\*\*\* $p < 0.0001$ , N.S. = not significant.

The %C3b<sup>+</sup> values for both GM1 and Ceramide-PEG were highly donor-dependent (varying from below 10% to above 80%), whereas the C3b surface density was similar on GM1 and Ceramide-PEG liposomes (Figure 6e and 6f). The basic principle of complement is that any surface not specifically protected will be attacked, and cell membranes of the host are hence protected by complement inhibitors such as factor H.<sup>[63]</sup> Gangliosides works as ligands for factor H, and it may be this immunosuppressive “self-marker” capacity that prevents the opsonisation of the GM1 liposomes.<sup>[58,59,64,65]</sup> It has previously been demonstrated that GM1 does not form an efficient steric barrier, and based on that suggested that GM1 works through a dysopsonising mechanism.<sup>[66,67]</sup> Our results confirm that GM1 indeed cannot prevent C3b opsonisation. Interestingly, GM1 did still reduce the antibody generation against liposomes below the level observed for Naked liposomes (compare Figure 6a-d to Figure 2b and 2e), this suggests that antibody generation against liposomes is an event triggered even further downstream in the immune response, e.g. on a B cell level. Importantly, however, the *stealth* abilities imposed by GM1, was early on found to be very specific to mice, whereas GM1 liposomes did not show long circulation-times in rats.<sup>[68]</sup> Our findings with high C3b adsorption to a subpopulation of GM1 liposomes in human plasma thus corroborate previous bulk studies in rat plasma.<sup>[69]</sup> The discrepancies of GM1 liposome immunogenicity, when comparing IgG/IgM generation in mice and C3b adsorption in humans, could thus very well be due to biological differences between the species. Overall, these data illustrate the tight regulation and specificity of opsonization, as introducing a known biologically active self-marker in a liposomal membrane can strongly inhibit antibody generation against liposomes, whereas introducing an inert steric surface-barrier cannot.

## 2.4. Opsonization heterogeneity have different patterns for antibodies and complement

Examining opsonization of a plethora of liposome formulations using SLOM allowed us to also perform a deeper investigation of how changes in the number of opsonin-positive liposomes correlated with changes in the opsonin surface density when modifying liposome properties. Therefore, we plotted the average IgG or IgM surface density for the 100 nm subpopulation of the ensemble versus the %IgG<sup>+</sup> or %IgM<sup>+</sup> values (**Figure 7a and 7b**). It is evident that for liposome systems displaying increasingly larger moieties on their surface (DPPE < DPPE-Succinyl < Mifamurtide < Ceramide-PEG = DSPE-PEG) we first detect an increase in %IgG<sup>+</sup> or %IgM<sup>+</sup> values, and only when these reaches close to 100 % does the antibody surface density start to increase. The biologically active GM1 is a noteworthy exception. The antibody-generation patterns were similar when mice were exposed to single and multiple injections of liposomes (**Figure S17-S19**, Supporting Information). We also plotted the C3b surface density for the 100 nm subpopulation of all liposome systems versus the %C3b<sup>+</sup> values (**Figure 7c**). For the C3b data we also observed a surface-moiety size dependency, but the conjugates only notably increased the %C3b<sup>+</sup> value and not the surface density. Hence DPPE, GM1, DSPE-PEG and Ceramide-PEG liposomes have comparable C3b surface densities from 8-12, but mean %C3b<sup>+</sup> values ranging from  $9.7 \pm 5.3\%$  for DPPE to  $73.3 \pm 10.6\%$  for DSPE-PEG (**Figure 7c**). Overall these data suggest that increasing levels of opsonization found for various liposome formulations follows different patterns for antibodies and C3b. Antibodies follow a opsonization trend described in **Figure 7d** that, when increasing amounts of antibodies are generated, goes through stages of I) no association, II) low percentage of opsonin-positive liposomes and low surface density, IV) high percentage of opsonin-positive liposomes and low surface density, before reaching V) high percentage of opsonin positive liposomes and high surface density. On the contrary, as liposome immunogenicity increases, C3b opsonization follows a trend of association that goes through stages of I) no association, III) low percentage

of opsonin-positive liposomes and high surface density, and then V) high percentage of opsonin-positive liposomes and high surface density (Figure 7c and 7d).

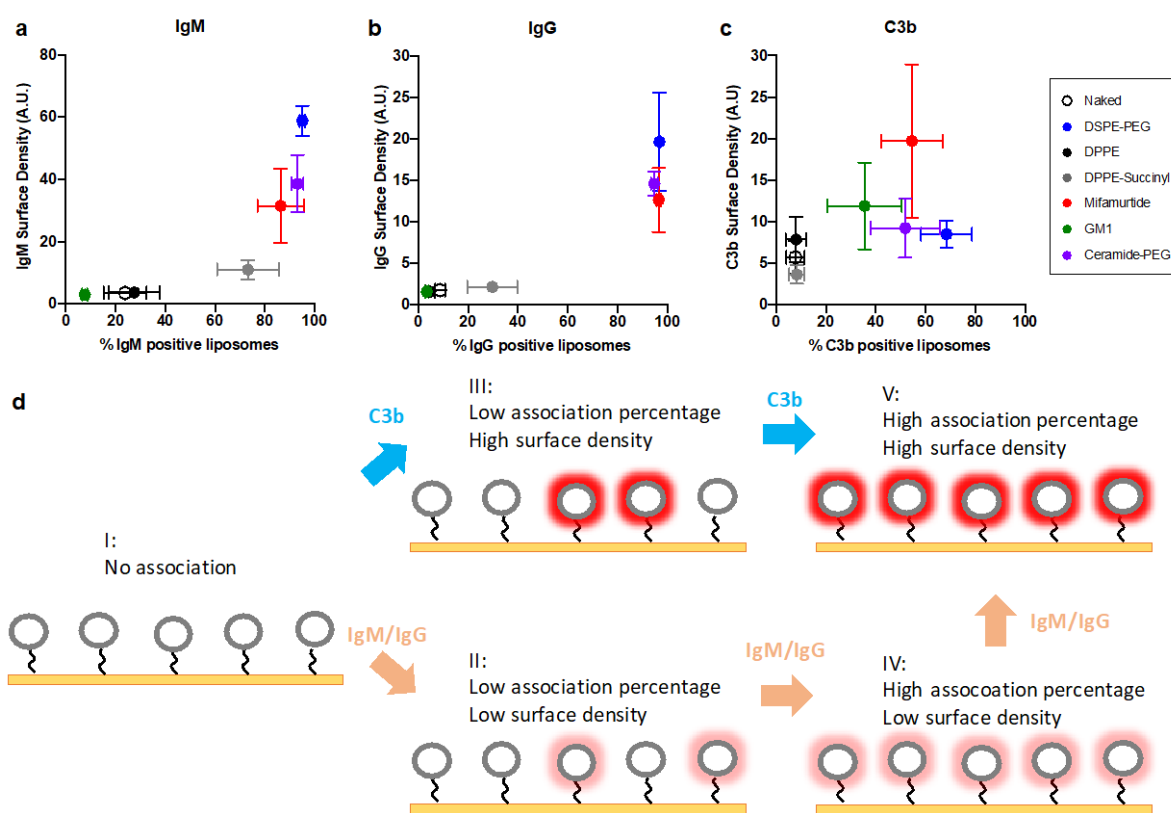


**Figure 7.** Displaying surface moieties with increasing size leads to increased liposome opsonization through different mechanistic patterns for antibodies and C3b. a) The average IgM surface density for the 100 nm size bin (75-125 nm) is plotted as a function of the average %IgM+ value for all liposome systems studied in this piece of work. b) The average IgG surface density for the 100 nm size bin is plotted as a function of the average %IgG+ value for each individual mouse in the study. c) The average C3b surface density for the 100 nm size bin is plotted as a function of the average %C3b+ value for each individual human donor in the study. The color coding corresponds to the liposomal systems investigated. d) Scheme depicting the five main opsonization scenarios found using SLOM: (I) No detectable association (only observed in naïve mice and for GM1 liposomes), (II) low percentage opsonin positive liposomes with a low surface density, (III) low percentage opsonin positive liposomes with a high surface density (only observed for C3b) (IV), high percentage opsonin positive liposomes

with a low surface density. (V) high percentage opsonin positive liposomes with a high surface density. Importantly, scenario III and IV would be indistinguishable in a bulk assay. The data in a) – c) reveal that for liposomal system displaying progressively larger surface moieties, the opsonization is increased through different patterns for antibodies (I  $\rightarrow$  II  $\rightarrow$  IV  $\rightarrow$  V, orange arrows) and C3b (I  $\rightarrow$  III  $\rightarrow$  V, blue arrows).  $N = 4-6$ , error bars show SEM of donor variation.

Interestingly, these observations with non-uniform distribution of C3b on the liposomes in the ensemble corroborate the known biological mechanism of the complement opsonization machinery: Complement works as a positive feedback mechanism through self-activation, where a nucleation event with one adsorbed C3b molecule can facilitate complete coating of a surface through the so-called “amplification loop”.<sup>[52]</sup> We here display for the first time that initiation of complement cascade will lead to substantial C3b surface-densities on individual liposomes while leaving other liposomes non-opsonized. Initiation of complement on liposomal surfaces has earlier been proposed to be mediated by antibodies,<sup>[8,40]</sup> but ~~whereas our isolation-based bulk approach gave similar indications (Figure S20, Supporting Information), the~~ homogeneous association patterns of antibodies were remarkably different from the heterogeneous association pattern of C3b (Figure 7). This indicates that antibodies and C3b follows distinctly different opsonization mechanisms and may not be directly linked as found using bulk assays.<sup>[8,40]</sup>

**2.5. PEGylation does not reduce opsonization** Using minimally invasive conditions, we provide the first direct visual evidence of single liposome opsonization, showing that PEGylation does not reduce opsonization as originally proposed.<sup>[6,70]</sup> On the contrary, PEGylation of liposomes substantially increased C3b adsorption (Figure 3). In addition, while almost no anti-liposome antibodies were detected in mice not previously exposed to liposomes for any of the liposomal surface architectures in the study (Figure S8 and S14, Supporting

Information), PEGylated liposomes were those with the highest antibody generation in the study after both single (Figure S17-S19, Supporting Information) and multiple exposures (Figure 7). Using Size Exclusion Chromatography and LC-MS/MS, we investigated adsorption of a broad range of opsonins<sup>[71]</sup> to PEGylated and Naked liposomes, and for none of them did we observe that PEG significantly reduced the opsonization (**Figure S20**, Supporting Information). This supports recent reports that the long-circulating properties achieved by PEGylation is not due to a steric barrier reducing opsonin association, instead suggesting an increase in dysopsonins, i.e. proteins that inhibit phagocytosis (**Figure S21**, Supporting Information).<sup>[16,71]</sup> Our data thus add to the emerging realization that neither stealth properties nor overall low-fouling (protein-repellent) properties correlate with C3b opsonization.<sup>[14,15]</sup> This strongly indicate that *stealth* properties are either independent of the complement system, or that they happen downstream of the initial C3b deposition, e.g. through inactivation or inhibition of the bound C3b, or by preventing binding of C3b to complement receptors.

The systematic study presented here, investigating opsonization by three types of opsonins on seven different liposome compositions, allowed us to pinpoint the molecular features of the PEG-lipid that facilitated opsonization. We demonstrated that association of antibodies and C3b was independent of the structure of the anchor group, and that the phosphoethanolamine linker group only had minor effects on immunogenicity. However, opsonization was highly dependent on the presentation of the PEG-moiety on a liposomal surface. Interestingly, strong opsonization was not restricted to liposomes prepared with PEGylated lipids, but was also observed for liposomes functionalized with lipid-conjugated drugs. This indicates that antibody and complement opsonization is a generic surface effect induced by large moieties displayed in a repeated pattern on a liposomal surface. Our results thus imply that simply shifting to alternative hydrophilic polymer-conjugates believed to provide a steric barrier<sup>[72]</sup> might not be a viable strategy if immunogenic reactions towards liposomes are to be avoided. Instead,

modifying liposomes with immunosuppressive self-markers could be a superior strategy for preparing *stealth* liposomes that maintain their long-circulating properties upon repeated administration.<sup>[23]</sup>

## 2.6. Benefits and limitations of the SLOM assay

The modifiable nature of the SLOM assay allows for detecting adsorption of a wide panel of proteins to liposomes, simply requiring a fluorescently labelled detection antibody specific against the protein of interest. Additionally, opsonization mediated by any type of component in liposomal membranes can be studied with SLOM using very low material consumption (5  $\mu$ L plasma, 0.2 nmol total lipid and 2  $\mu$ g detection antibodies per sample in the current setup). Furthermore, the SLOM assay allows for gaining insights into opsonisation heterogeneity, which as highlighted above is not possible with regular bulk assays relying on isolation of liposomes from plasma followed by proteomics. In addition, if only information about a single protein species is required, the experimental time is no longer than the time required to run a SEC column. For studying binding of multiple proteins, proteomic methods relying on LC-MS/MS has a much higher throughput than the SLOM method, however the commonly applied methods for isolation of liposomes from plasma, such as SEC and centrifugation, suffers from contaminations with unbound proteins.<sup>[73]</sup> these contamination issues can be largely eliminated when using a direct imaging-based setup.

Performing the SLOM assay using identical detection antibodies and microscope imaging settings allows for a direct comparison between experiments of the percentage of opsonin-positive liposomes and the opsonin surface density between experiments. Thus, for liposome systems with various surface-architectures the relative difference in opsonin generation and binding can be semi-quantitatively compared. The assay could be expanded to determine how this overall relative difference translates to the specific number of proteins per liposomes using

a method akin to the one presented by Belfiore *et al.* who determined the number of protein ligands on individual liposomes using stepwise photo bleaching.<sup>[74]</sup> Here, the stochastic bleaching of individual fluorophores will, when only a limited number remain, result in a stepwise decrease in fluorescence emission in the protein channel. If the number of fluorophores per protein is known, the exact number of proteins per particle can be determined by dividing the total emission intensity by the intensity of each bleaching step.<sup>[75]</sup> While such quantification is indeed essential for accurately characterising e.g. the number of targeting ligands on individual liposomes, for a comparative study on the opsonin binding between different liposome systems as the one presented here, it would not provide information greatly influencing the overall conclusions.

A characteristic of any antibody-based detection assay is that it only allows for measuring the presence of a protein, if the epitope recognized by the detection antibody is presented to the surrounding environment and not hidden in the protein/liposome interface. In contrast, proteomics-based setups can reveal the presence of the protein no matter how it is oriented, as well as if it is hidden below a layer of other proteins (an unlikely situation for PEGylated liposomes, however, due to their overall sparse protein binding<sup>[28]</sup>). This feature of the SLOM assay however also opens up new possibilities, as it allows for studying orientation of the bound proteins,<sup>[36]</sup> and whether e.g. the part of the protein binding the corresponding Fc- or C3-receptor on phagocytes is available for interactions. To ensure that antibody-based detection is not biased by epitope matching, it is important to perform an adequate control, which is why we made sure that the results presented in this work did not change if detection antibodies recognizing a different epitope on the opsonin was used (Figure S8, Supporting Information).

In the present work, a regular confocal microscope is applied. Hence, the individual liposomes appear as diffraction-limited spots, and only inter-particle heterogeneity can be studied, which

for the questions asked in the current work is sufficient. However, if applying super-resolution microscopy to study the setup in Figure 1a, intra-particle heterogeneity (i.e. distribution of proteins on the particle surface) could in principle be possible, at least for the largest liposomes. While Feiner-Gracia *et al.* presented spatial information of the protein corona of silica nanoparticles using STORM,<sup>[34]</sup> this may be more challenging for liposomes where lipids can diffuse laterally in the liposomal membrane and the protein corona hence also may be spatially dynamic. Electron microscopy could also be used for studying protein binding to nanoparticles with even higher resolution. While this method is even more low-throughput than SLOM due to more tedious sample preparation and requires more specialized equipment, it would allow for information on precise spatial arrangement of bound proteins.<sup>[36]</sup> While detection antibodies can be specifically labelled using gold particles, distinguishing the liposomes from other lipid particles in plasma can be challenging. Hence, specific labelling of the liposomes with other elements than gold will be required as well, in addition to and the use of more advanced EM techniques for distinguishing the liposome and antibody labels, such as energy-dispersive X-ray analysis.<sup>[76]</sup> Despite the lower resolution, the SLOM assay presented here hence offers the relevant information about inter-particle heterogeneity, employing standard confocal microscopy and off-the-shelf reagents.

## **2.7. The importance of addressing opsonization heterogeneity**

It is increasingly recognized that elucidating and understanding the potential hidden heterogeneities within nanomedicine might be a cornerstone for overcoming the translational gap currently limiting drug delivery research.<sup>[77,78]</sup> Here, we developed an assay capable of revealing considerable opsonization heterogeneity between individual liposomes. Our finding of distinct liposome subpopulations – one opsonin positive and another opsonin negative – represent a binding behaviour that has not previously been observed for opsonization, but has been described for other membrane interacting proteins binding to liposomes from solution,

albeit in less complex environments.<sup>[32,79,80]</sup> The origin of this phenomenon is yet to be fully understood,<sup>[32]</sup> but could be tied to heterogeneities in lipid composition<sup>[41,47]</sup> or PEGylation degree.<sup>[44]</sup> Heterogeneous opsonization is undetectable by bulk assays,<sup>[32]</sup> which assume all bound protein to be homogeneously distributed between the liposomes. However, a scenario with 20% opsonin-positive liposomes would give a five-fold underestimation of the *de facto* protein density per liposomes in a bulk assay. The functional performance of liposomal formulations could be affected by heterogeneous opsonization, since opsonization is directly linked to important parameters such as stability, clearance, targeting ability and ultimately therapeutic efficacy.<sup>[1,11,81,82]</sup> In a best case scenario a highly opsonized liposome subpopulation will lead to this population just having limited therapeutic effect, while a more severe side-effect of the subpopulation could be anaphylaxis and hypersensitivity reactions.<sup>[10,11,83]</sup> Hence, characterising nanoparticle opsonization at the single particle level is essential for designing more controllable, safe and efficient drug delivery systems.

### 3. Conclusion

In summary, the single liposome analysis allowed us to describe the full opsonization landscape and delineate how liposomal surface architectures affected both the number of opsonin-positive liposomes and the opsonin surface density on these. The assay demonstrated that PEG does not prevent opsonization with complement C3b but facilitates it, and that antibodies are generated against PEGylated liposomes but not non-PEGylated. Further, our findings suggested that such induction of opsonization is a general property for liposomal surface decorations, and not solely for PEG. The single-particle resolution of the SLOM assay also revealed the existence of liposome subpopulations with high protein adsorption, which could demonstrate deviant behaviour with respect to circulation properties and immunogenicity. SLOM hence allowed for a deeper understanding of liposomal protein-adsorption heterogeneity and how this is linked to liposomal surface architecture.

#### 4. Methods

*Materials:* All chemicals for the HEPES buffer, inductively coupled plasma mass spectrometry (ICP-MS) diluent, and zeta-potential buffer were acquired from Sigma Aldrich (Brøndby, Denmark). 1,2- Distearoyl-sn-glycero-3-phosphocholine (DSPC), 1,2-distearoyl-sn-glycero-3-phospho-ethanolamine- N-[methoxy (polyethylene glycol)-2000] (DSPE-PEG2000), 1,2-dipalmitoyl-sn-glycero-3-phospho- ethanolamine-N-(succinyl) (DPPE-Succinyl), N-palmitoyl-sphingosine-1-succinyl[methoxy(poly-ethylene glycol)2000] (Ceramide-PEG) and distearoyl-rac-glycerol-methoxy (polyethylene glycol)- 2000]) (DSG-PEG2000) were acquired from Avanti Polar Lipids (Alabaster, AL, US). Cholesterol was acquired from Lipoid (Ludwigshafen, Germany). Muramyl tripeptide phosphatidylethanolamine (Mifamurtide) and Monosialoganglioside extracted from bovine brain (GM1) was acquired from Sigma Aldrich. 1,1'-Dioctadecyl-3,3,3',3'-tetramethylindodicarbocyanine (DiD) was acquired from Thermo Fisher Scientific (Waltham, MA, US). AF488 labelled anti-IgM (Goat anti-Mouse IgM (Heavy chain) Cross-Adsorbed Secondary Antibody, catalogue number A-21042) and anti-IgG (Goat anti-Mouse IgG (H+L) Cross-Adsorbed Secondary Antibody, catalogue number A-11001) was acquired from Thermo Fisher Scientific. LPS from *S. Typhose* was acquired from Sigma Aldrich. FITC-labelled anti-human iC3b/C3b clone 10C7 (catalogue number CL7632F) was acquired from Cedarlane (Burlington, Ontario, Canada), clone 3E7 (catalogue number 846102) was acquired from Biolegend (San Diego, California, USA). According to the manufacturer, all detection antibodies employed for studying IgM and IgG had a labelling efficiency of 6. BSA, BSA-Biotin and Streptavidin for the single liposome assays were acquired from Sigma Aldrich.

*Mice:* BALB/cJRj mice (Janvier) aged 8-13 weeks old were used for all experiments. Upon arrival, the mice were subjected to at least 1 week of acclimation. Mice were kept under

controlled environmental conditions (constant temperature and humidity as well as a 12h:12h light:dark cycle). All experimental procedures were approved by the institutional ethical board and the Danish National Animal Experiment Inspectorate (licence number 2016-15-0201-00920, approved on 5<sup>th</sup> of July 2016). Liposomes were, for all experiments in the main manuscript, administered intravenously in the tail vein on a q4d schedule for a total of two injections (day 1 and 4). Blood samples were collected in hirudin blood tubes (Roche) on day 8. Samples were centrifuged at 2000 g for 15 min at 4 °C and resulting plasma fractions were collected in Protein LoBind Eppendorf tubes (Eppendorf, Hamburg, Germany) and stored at -80 °C until SLOM analysis. Exposing mice to only one single injection and collecting plasma after 8 days, did not change the outcome of the experiments (Figure S11-S13, Supporting Information).

*Collection of human plasma:* Human plasma was collected as previously described<sup>[84]</sup>. Briefly, blood was drawn by certified staff from healthy donors under signed consent. The identities of the donors were unknown to the researchers performing the experiments and all requirements for blood collection at the Technical University of Denmark was followed in agreement with the guidelines of National Committee on Health Research Ethics. Blood was collected in Hirudin tubes (Sarstedt, Nürnbrecht, Germany). The blood was transferred to 2 mL Protein LoBind Eppendorf tubes (Eppendorf, Hamburg, Germany) and centrifuged at 3000 g for 15 minutes in order to separate cells from plasma. The plasma supernatant was transferred to fresh LoBind tubes and stored at 4 °C. Experiments with human plasma were always carried out on the same day as the blood was drawn, and remaining biological material destroyed afterwards.

*Liposome preparation:* Liposomes were prepared and characterized as previously described<sup>[85]</sup>. Briefly, lipids in powder forms were dissolved in tert-butanol:MQ water 9:1, mixed to the desired lipid compositions in glass vials and freeze-dried overnight. The dry lipids were re-

hydrated in HEPES buffer (10 mM HEPES, 150 mM NaCl buffer, pH 7.4) to a concentration of 50 mM total lipid and put under 65 °C heating and magnet stirring for minimum 1 h. The size of the liposomes were controlled by extruding 21 times through a 100 nm Whatman filter (GE Healthcare, Little Chalfont, UK) using an Avanti mini-extruder (Avanti Polar Lipids) on a heating block at 65 °C. The liposomes were transferred to a new glass vial and stored at 4 °C. The composition of the PEGylated liposomes were DSPC:Cholesterol:DSPE-PEG2000 (molar ratio 56.6:38.2:5.2). In Naked liposomes, the DSPE-PEG was replaced by DSPC. In formulations with DPPE-Succinyl, Mifamurtide, GM1, DSG-PEG and Ceramide-PEG, the DSPE-PEG was replaced by 5.2 mol% of the respective lipids. In SLOM liposomes, 0.2 mol% DiD and 0.05 mol% DSPE-PEG2000-Biotin (Avanti Polar Lipids) were added to the formulations. The amount of DiD incorporated into the lipid mixture is based on the wish to make sure there is enough DiD molecules per liposome to avoid liposome-to-liposome variations being affected by Poisson statistics, as well as ensuring a good signal-to-noise ratio of the detection signal. However, the amount DiD in the liposomes should also be kept low enough to avoid intra-liposome quenching as this would bias the liposome intensity to size conversion, and because a too high DiD concentration could affect the physicochemical properties of the liposomes. The use of 0.2 mol% lipid-fluorophore has previously been shown to fulfill the criteria outlined above.<sup>[41,43]</sup>

Total lipid concentration of the liposome stocks was determined by measuring the phosphorus concentration using ICP-MS. Samples were diluted 10,000 times in an ICP-MS diluent (2% HCl, 10 ppb Ga) to fall within a standard range of 25-100 ppb phosphorus, and the phosphorus content was measured on an ICAP-Q from Thermo Fisher Scientific. The lipid concentration was calculated based on the assumption that 61.8 % of the lipids in our formulations contain a phosphorus atom.

The hydrodynamic diameter and polydispersity index (PDI) of the liposomes were measured by dynamic light scattering (DLS) using a ZetaSizer Nano ZS from Malvern Instruments

(Malvern, Worcestershire, UK), equipped with a 633 nm laser. The liposomes were diluted to about 120  $\mu\text{M}$  total lipid in HEPES buffer, and the size measured as the average from 3 runs of 15 cycles. The zeta potential of the liposomes was measured using the same instrument by M3-PALS in glucose buffer (300 mM glucose, 10 mM HEPES, 1 mM  $\text{CaCl}_2$  at pH 7.4) at 120  $\mu\text{M}$  total lipid. Each measurement consisted of 3 individual runs in automatic mode (10-100 cycles). Characteristics are shown in Table S1.

*Single Liposome Opsonization Measurement (SLOM):* To image individual liposomes we followed previously published protocols,<sup>[41–43,47]</sup> allowing us to tether single liposomes on a passivated glass surface and image them using confocal microscopy. In brief, each chamber in an Ibidi  $\mu$ -slide 8 well glass coverslips for microscopy (Ibidi, Martinsreid, Germany) was incubated with a 1 mg  $\text{mL}^{-1}$  1:10 mixture of BSA-Biotin:BSA for 20 minutes at room temperature. After washing 8 times with HEPES buffer, each chamber was incubated with 25  $\mu\text{g mL}^{-1}$  Streptavidin for 10 minutes, followed by eight additional washes with HEPES buffer. Liposomes were diluted to a final concentration of 1  $\mu\text{M}$  lipid and added to chambers on the coverslip. Unbound liposomes were removed by washing the plate in HEPES buffer after incubating for 3 minutes. It has previously been verified the immobilization does not influence liposome shape.<sup>[86]</sup>

Next, plasma was diluted 1:40 in HEPES buffer, added to the well and allowed to incubate with the immobilised liposomes for 10 minutes. Following 4 washes with HEPES buffer, secondary AF488-labelled antibodies against the respective antibody of interest (mouse IgG or IgM) were diluted to 10  $\mu\text{g mL}^{-1}$  and added to the well. IgG binding was assessed using Goat anti-Mouse IgG (H+L) Cross-Adsorbed Secondary Antibody (Invitrogen) while IgM binding was assessed using Goat anti-Mouse IgM (Heavy chain) Cross-Adsorbed Secondary Antibody (Invitrogen). For detection of C3b binding, primary FITC-labelled antibodies against C3b/iC3b were diluted to 2.5  $\mu\text{g mL}^{-1}$  and added to the well. With 6-8 fluorophores per antibody according to the

manufacturer, single antibodies should be possible to detect. Non-specific binding of the detection antibodies to the liposomes was not detected (see Figure S9 and Figure S10, Supporting Information), and no precautions were hence necessary for blocking non-specific binding. After further 10 minutes incubation, unbound antibodies were removed and the plate washed three times in HEPES buffer before imaging the liposomes.

The reason for using the 1:40 plasma dilution in the current study is mainly practical: In order to completely cover the bottom of the Ibidi microscopy wells, approx. 200  $\mu$ L of liquid is required. Due to the relatively small blood volume of mice, the plasma samples available were rarely more than 50  $\mu$ L. Additionally, as the plasma sample from one animal was often used for several experiments (e.g. for the competition assay in Figure 4 and for studying cross-interactions in Figure S7, Supporting Information), not even a 1:4 or 1:10 dilution was practical. Instead, 5  $\mu$ L mouse plasma was consistently diluted in 195  $\mu$ L HBS. However, there are no experimental limitations preventing performing the assay in 100 % serum.

Competition with PEG was done by pre-incubating the plasma for 10 minutes at RT in a Protein LoBind tube with either mPEG2000 (Sigma), DSPE-PEG2000 micelles or DSPC:Cholesterol:DSPE-PEG2000 liposomes at the stated concentrations. For liposomes, the PEG concentration was calculated based on the assumption that 50% of the total DSPE-PEG content was presented in the outer leaflet of the membrane. DSPE-PEG micelles were prepared by diluting the lipid in HEPES buffer and solubilizing the phospholipids by 30 minutes of ultra-sonication. The size of the micelles was determined with DLS to be 10-15 nm. For the graphs in Figure 4, the binding percentage and surface density in presence of competition particles was normalized to the respective value in absence of competition particles. This was done for all five size groups. Error bars show the variation between the five size groups.

For imaging liposomes, we used a Leica TCS SP5 inverted confocal microscope equipped with an oil immersion objective HCX PL APO CS  $\times$  100 (Numerical Aperture 1.4) (Leica Microsystems, Wetzlar, Germany). Detection of AF488 was performed at 495–580 nm

(excitation at 488 nm), while detection of DiD was performed at 645–800 nm (excitation at 633 nm) using photo-multipliers. In all cases, sequential imaging was used to avoid cross excitation. Images had a resolution of  $1024 \times 1024$  pixels, with a pixel size of 50.5 nm and a bit depth of 16. All experiments were performed at RT. For the current study, all imaging was performed within a few months using the same microscope and the instrument settings (such as laser power, PMT settings etc.). By confirming that the DiD fluorescence intensities of the same liposome formulations did not change between different experimental dates, it was found that no internal calibration was needed. If comparing data from different microscopes or detection antibodies measured on different lasers, we would however recommend imaging fluorescent calibration beads and normalize the measured fluorescence intensities to these. Image analysis and data treatment were performed using the ComDet plugin in Fiji (ImageJ), which allowed for identifying and localizing the liposomes and extracting the DiD fluorescence intensity of each liposome, as well as the AF488 intensity co-localized with the liposome.

As previously published,<sup>[46–48,87]</sup> the integrated intensity of the liposome membrane dye can be converted to diameter, since the integrated intensity of the DiD membrane label is proportional to the number of membrane dyes, which scales with the surface area. The liposome diameter is consequently proportional to the square root of the integrated intensity, scaled by a calibration factor. The calibration factor is obtained by DLS and correlated to the mean integrated intensity calculated from an intensity histogram of the confocal images of the liposomes. Previous control experiment using electron microscopy have shown that the integrated intensity-based liposome size conversion is not significantly biased by multi-lamellar liposomes as the presence of these is negligible (<5 %).<sup>[43]</sup> Furthermore, previous single liposome characterization experiments with liposomes containing pre-mixed pairs of fluorophores have shown that significant curvature-dependent sorting of the liposome reporter lipid-fluorophore (like DiD) does not occur, and hence that the molar percentage of lipid fluorophore in the individual liposome does not depend on the size of the liposome.<sup>[41,88]</sup> Finally, the method for converting

integrated liposome intensity signals to liposome diameters have previously been rigorously established and benchmarked against classical methodologies such as electron microscopy and DLS, estimating a  $\pm 5$  nm uncertainty on the liposome diameter determined by the fluorescence approach.<sup>[46,87]</sup> For each liposome the integrated AF488 or FITC intensity scales with the number of detection antibodies bound to the liposome, and hence the number of adsorbed opsonins. Thus, the AF488/DiD intensity ratio gives us the absolute density in arbitrary units. Data filtering into size groups was done using Excel. Statistical analysis was performed in GraphPad Prism.

In order for the immobilized liposomes to accurately represent the structure of the non-immobilized nanocarrier, we ensured to follow previously established protocols for executing the single liposome assay,<sup>[41–43,47]</sup> where a plethora of control experiments have confirmed the liposome structural integrity upon surface immobilization. It has previously been shown that liposomes display negligible non-specific surface interaction as no immobilization was observed when the streptavidin linker was absent.<sup>[43]</sup> Additionally, liposomes with encapsulated fluorescent molecules do not display leaking upon immobilization, confirming that liposome are intact (do not rupture or fuse) on the surface.<sup>[89]</sup> Finally, FRET patterns between immobilized liposomes and supported lipid bilayers helped confirm that surface immobilization of liposomes through streptavidin-biotin coupling can be fine-tuned to avoid detrimental liposome:surface interactions, hereby preserving the spherical shape of liposomes.<sup>[86]</sup>

*Separation of liposome-bound from free C3b using SEC:* In order to quantify the binding of plasma proteins to liposomes, Naked or DSPE-PEG liposomes labelled with 0.1% DSPE-Cy5 (Avanti Polar Lipids) were diluted in fresh human plasma to a final concentration of 2 mM total lipid and approx. plasma concentration of 95%. As a control, plasma diluted to 95% with HEPES buffer was used. After 1 h incubation, the sample (1 mL) was applied to size exclusion chromatography (SEC) columns. SEC was performed using a Sepharose CL-4B matrix (GE

Health- care, Little Chalfont, UK) packed in 50 cm Econo-Column glass chromatography columns purchased from Bio-Rad (Hercules, CA, USA) with PBS as mobile phase. The flow was kept at  $0.5 \text{ mL min}^{-1}$  using a Masterflex peristaltic pump (Cole Parmer, Illinois, USA). The first 24 mL eluting from the column were allowed to run into the waste before initiating collection of fractions. 24 1-mL fractions were collected before allowing the free plasma proteins to elute into the waste. The column was then left to clean for 105 minutes before adding the next sample. 125  $\mu\text{L}$  of each fraction were loaded into a black 96-well plate and the liposome eluting profile determined using the DSPE-Cy5 fluorescence (excitation at 649nm and reading emission at 666nm) and comparing to a standard range of the corresponding liposomes. The protein concentration in the samples was determined by reading the protein auto-fluorescence (excitation at 295nm and reading emission at 345nm) and comparing to a BSA standard range. Fluorescence readout was done using a TECAN Spark microplate reader. For each sample, fractions containing  $>7.5\%$  of the total eluting DSPE-Cy5 was pooled into one sample. Samples from different donors were analysed separately.

*Quantitative tandem mass spectrometry:* LC-MS/MS was used to identify and quantify proteins bound to the liposomes after separation of liposomes with their biomolecular corona from complete plasma using SEC. This was done using previously established protocols for protein corona characterization.<sup>[28,73]</sup> First, 250  $\mu\text{L}$  of the samples under investigation were mixed with lysis buffer (5% sodium deoxycholate, 50 mM triethylammonium bicarbonate, pH 8.5, 250  $\mu\text{L}$ ) in Protein LoBind Eppendorf tubes. The samples were then incubated at  $95^\circ\text{C}$  for 5 min for denaturation of the proteins. Subsequently, the samples were transferred to a Microcon-10kDa centrifugal filter unit (Merck) and centrifuged at 14,000 g until the solvent had flown through the filter. After discarding the filtrate, the samples were reduced and alkylated at 10 mM tris(2-carboxyethyl)phosphine, 50 mM 2-chloroacetamide in digestion buffer (0.5% sodium deoxycholate, 50 mM triethylammonium bicarbonate, pH 8.5, 200  $\mu\text{L}$ ). The samples were

incubated for 30 min at 37 °C followed by another centrifugation at 14,000 g until the solvent had flown through the filter. The filtrate was discarded, and the samples were washed by adding 200 µL digestion buffer, followed by another centrifugation (14,000 g). The inner spin filters were transferred to new collection tubes, and Pierce Trypsin Protease, MS Grade (Thermo Scientific) in digestion buffer was added to the filters in a protein:trypsin ratio of 50:1. The samples were vortexed and incubated overnight at 37 °C to digest the proteins. The following morning, the samples were centrifuged at 14,000 g until the protein digest had flown through the filters. To ensure complete recovery of the protein digest, 50 mM triethylammonium bicarbonate buffer (100 µL, pH 8.5) was added to the filters, and the filters were centrifuged at 14,000 g until the buffer had flown through the filters and into the collection tubes. Next, ethyl acetate extraction was performed by adding ethyl acetate (450 µL) and trifluoroacetic acid (7.5 µL) to all tubes. The tubes were vortexed and centrifuged at 14,000 g for 5 min to obtain phase separation. The top organic phase, containing the sodium deoxycholate and phospholipids, was removed by pipette to get rid of the sodium deoxycholate. Additional ethyl acetate (450 µL) was added to all samples and the procedure was repeated, thus attaining the bottom phase, containing the peptides only. Each sample was then dried in a vacuum centrifuge and resuspended in 30 µL 2% acetonitrile (MeCN), 0.1% trifluoroacetic acid (TFA), 0.1% formic acid (FA) aqueous solution. The samples were vortexed, spun down using a minicentrifuge, and ultrasonicated for 2 min. Subsequently, the samples were spun down at 14,000 g, 8 µL of the supernatant loaded into a 96-well plate and spiked with a total of 100 fmol MS Qual/Quant QC Mix (Sigma Aldrich), yielding a total volume of 10 µL, which was all injected.

The samples were investigated in technical duplicate using a UPLC-nanoESI MS/MS setup consisting of a Dionex RSLC nanopump (Dionex RSLC 3500, Thermo Fisher Scientific) connected to a Q Exactive HF-X-Hybrid Quadrupole-Orbitrap mass spectrometer (Thermo Fisher Scientific). The peptide samples were loaded onto a C18 reversed phase precolumn (Dionex Acclaim PepMap RSLC C18, 2 µm, 100 Å, 100 µm × 2 cm) and separated on a 50 cm

analytical C18 Micro pillar array column ( $\mu$ PAC, PharmaFluidics) at 30 °C with a constant flow rate of 0.75  $\mu$ L min<sup>-1</sup>. The mobile phases were (A) water with 2% MeCN and 0.1% FA and (B) MeCN with 0.1% FA. The loading was done with 2% B over 5 min. The separation was performed by a linear gradient from 8% B to 30% B over 35 min. All solvents were MS-grade. A full MS scan in the mass range of  $m/z$  375 to 1200 was acquired at a resolution of 120,000. The precursor ions were isolated using a quadrupole isolation window of  $m/z$  1.6 and fragmented using higher-energy collision dissociation (HCD) with a normalised collision energy of 28. Fragmented ions were dynamically added to an exclusion list for 15 s. All acquired MS scans were searched using default settings in MaxQuant/Andromeda 1.6.10.43., against a human reference database (Uniprot, proteins entries: 20.368, accessed 20/10-2019). Standard settings were employed with carbamidomethyl (C) as a static modification and protein N-terminal acetylation, deamidation (NQ) and oxidation (M) as variable modifications. Protein identification was reported at a FDR of 1%, with identification match between runs toggled on. The MaxQuant results were processed using Perseus 1.6.10.43. One or more unique peptides in at least one group were required for protein quantification using LFQ. Proteins identified solely by site as well as reverse peptides were removed from the results. Keratins were considered to be contaminants, and were also removed from the final list of proteins.

### Supporting Information

Supporting Information is available from the Wiley Online Library or from the author.

### Acknowledgements

The work was supported by the Novo Nordisk Foundation (Grant No NNF16OC0022166). The Danish National Mass Spectrometry Platform for Functional Proteomics (PRO-MS: grant no. 5072-00007B) and the Svend Andersen Foundation are acknowledged for parts of this study.

Received: ((will be filled in by the editorial staff))

Revised: ((will be filled in by the editorial staff))

Published online: ((will be filled in by the editorial staff))

## References

- [1] M. P. Monopoli, C. Åberg, A. Salvati, K. A. Dawson, *Nat. Nanotechnol.* **2012**, *7*, 779.
- [2] R. Cai, C. Chen, *Adv. Mater.* **2019**, *31*, 1805740.
- [3] O. Nag, V. Awasthi, *Pharmaceutics* **2013**, *5*, 542.
- [4] M. L. Immordino, F. Dosio, L. Cattel, *Int. J. Nanomedicine* **2006**, *1*, 297.
- [5] Y. (Chezy) Barenholz, *J. Control. Release* **2012**, *160*, 117.
- [6] D. D. Lasic, F. J. Martin, A. Gabizon, S. K. Huang, D. Papahadjopoulos, *Biochim. Biophys. Acta - Biomembr.* **1991**, *1070*, 187.
- [7] J. J. F. Verhoef, J. F. Carpenter, T. J. Anchordoquy, H. Schellekens, *Drug Discov. Today* **2014**, *19*, 1945.
- [8] V. P. Vu, G. B. Gifford, F. Chen, H. Benasutti, G. Wang, E. V. Groman, R. Scheinman, L. Saba, S. M. Moghimi, D. Simberg, *Nat. Nanotechnol.* **2019**, *14*, 260.
- [9] A. Judge, K. McClintock, J. R. Phelps, I. MacLachlan, *Mol. Ther.* **2006**, *13*, 328.
- [10] G. T. Kozma, T. Mészáros, I. Vashegyi, T. Fülöp, E. Örfi, L. Dézsi, L. Rosivall, Y. Bavli, R. Urbanics, T. E. Mollnes, Y. Barenholz, J. Szebeni, *ACS Nano* **2019**, *13*, 9315.
- [11] A. Gabizon, J. Szebeni, *ACS Nano* **2020**, *14*, 7682.
- [12] M. Mohamed, A. S. Abu Lila, T. Shimizu, E. Alaaeldin, A. Hussein, H. A. Sarhan, J. Szebeni, T. Ishida, *Sci. Technol. Adv. Mater.* **2019**, *20*, 710.
- [13] T. Ishida, H. Kiwada, *Int. J. Pharm.* **2008**, *354*, 56.
- [14] N. Bertrand, P. Grenier, M. Mahmoudi, E. M. Lima, E. A. Appel, F. Dormont, J.-M. Lim, R. Karnik, R. Langer, O. C. Farokhzad, *Nat. Commun.* **2017**, *8*, 777.
- [15] A. C. G. Weiss, H. G. Kelly, M. Faria, Q. A. Besford, A. K. Wheatley, C.-S. Ang, E. J. Crampin, F. Caruso, S. J. Kent, *ACS Nano* **2019**, *13*, 4980.
- [16] S. Schöttler, G. Becker, S. Winzen, T. Steinbach, K. Mohr, K. Landfester, V. Mailänder, F. R. Wurm, *Nat. Nanotechnol.* **2016**, *11*, 372.
- [17] *Nat. Biotechnol.* **2014**, *32*, 961.

- [18] S. Wilhelm, A. J. Tavares, Q. Dai, S. Ohta, J. Audet, H. F. Dvorak, W. C. W. Chan, *Nat. Rev. Mater.* **2016**, *1*, 16014.
- [19] V. J. Venditto, F. C. Szoka, *Adv. Drug Deliv. Rev.* **2013**, *65*, 80.
- [20] T. Ishida, X. Wang, T. Shimizu, K. Nawata, H. Kiwada, *J. Control. Release* **2007**, *122*, 349.
- [21] X. Wang, T. Ishida, H. Kiwada, *J. Control. Release* **2007**, *119*, 236.
- [22] M. D. McSweeney, L. S. L. Price, T. Wessler, E. C. Ciociola, L. B. Herity, J. A. Piscitelli, A. C. DeWalle, T. N. Harris, A. K. P. Chan, R. S. Saw, P. Hu, J. C. Jennette, M. G. Forest, Y. Cao, S. A. Montgomery, W. C. Zamboni, S. K. Lai, *J. Control. Release* **2019**, *311–312*, 138.
- [23] Y. Mima, A. S. Abu Lila, T. Shimizu, M. Ukawa, H. Ando, Y. Kurata, T. Ishida, *J. Control. Release* **2017**, *250*, 20.
- [24] H. Schellekens, W. E. Hennink, V. Brinks, *Pharm. Res.* **2013**, *30*, 1729.
- [25] Q. Yang, S. K. Lai, *Wiley Interdiscip. Rev. Nanomedicine Nanobiotechnology* **2015**, *7*, 655.
- [26] G. T. Kozma, T. Shimizu, T. Ishida, J. Szebeni, *Adv. Drug Deliv. Rev.* **2020**, *154–155*, 163.
- [27] C. Carrillo-Carrion, M. Carril, W. J. Parak, *Curr. Opin. Biotechnol.* **2017**, *46*, 106.
- [28] K. Kristensen, T. B. Engel, A. Stensballe, J. B. Simonsen, T. L. Andresen, *J. Control. Release* **2019**, *307*, 1.
- [29] J. B. Simonsen, R. Münter, *Angew. Chemie Int. Ed.* **2020**, *59*, 12584.
- [30] R. Pattipeiluhu, S. Crielgaard, I. Klein-Schiphorst, B. I. Florea, A. Kros, F. Campbell, *ACS Cent. Sci.* **2020**, *6*, 535.
- [31] S. M. Moghimi, D. Simberg, E. Papini, Z. S. Farhangrazi, *Adv. Drug Deliv. Rev.* **2020**, *157*, 83.
- [32] V. K. Bhatia, N. S. Hatzakis, D. Stamou, *Semin. Cell Dev. Biol.* **2010**, *21*, 381.

- [33] V. Forest, J. Pourchez, *Nano Today* **2016**, *11*, 700.
- [34] N. Feiner-Gracia, M. Beck, S. Pujals, S. Tosi, T. Mandal, C. Buske, M. Linden, L. Albertazzi, *Small* **2017**, *13*, 1701631.
- [35] S. Galmarini, U. Hanusch, M. Giraud, N. Cayla, D. Chiappe, N. von Moos, H. Hofmann, L. Maurizi, *Bioconjug. Chem.* **2018**, *29*, 3385.
- [36] P. M. Kelly, C. Åberg, E. Polo, A. O'Connell, J. Cookman, J. Fallon, Ž. Krpetić, K. A. Dawson, *Nat. Nanotechnol.* **2015**, *10*, 472.
- [37] A. M. Clemments, P. Botella, C. C. Landry, *J. Am. Chem. Soc.* **2017**, *139*, 3978.
- [38] U. Bulbake, S. Doppalapudi, N. Kommineni, W. Khan, *Pharmaceutics* **2017**, *9*, 12.
- [39] Y. Bavli, I. Winkler, B. M. Chen, S. Roffler, R. Cohen, J. Szebeni, Y. Barenholz, *J. Control. Release* **2019**, *306*, 138.
- [40] E. Chen, B.-M. Chen, Y.-C. Su, Y.-C. Chang, T.-L. Cheng, Y. Barenholz, S. R. Roffler, *ACS Nano* **2020**, *14*, 7808.
- [41] J. Larsen, N. S. Hatzakis, D. Stamou, *J. Am. Chem. Soc.* **2011**, *133*, 10685.
- [42] J. B. Larsen, M. B. Jensen, V. K. Bhatia, S. L. Pedersen, T. Bjørnholm, L. Iversen, M. Uline, I. Szleifer, K. J. Jensen, N. S. Hatzakis, D. Stamou, *Nat. Chem. Biol.* **2015**, *11*, 192.
- [43] N. S. Hatzakis, V. K. Bhatia, J. Larsen, K. L. Madsen, P.-Y. Bolinger, A. H. Kunding, J. Castillo, U. Gether, P. Hedegård, D. Stamou, *Nat. Chem. Biol.* **2009**, *5*, 835.
- [44] R. Eliassen, T. L. Andresen, J. B. Larsen, *Adv. Mater. Interfaces* **2019**, *6*, 1801807.
- [45] M. B. Pedersen, X. Zhou, E. K. U. Larsen, U. S. Sørensen, J. Kjems, J. V. Nygaard, J. R. Nyengaard, R. L. Meyer, T. Boesen, T. Vorup-Jensen, *J. Immunol.* **2010**, *184*, 1931.
- [46] A. H. Kunding, M. W. Mortensen, S. M. Christensen, D. Stamou, *Biophys. J.* **2008**, *95*, 1176.
- [47] R. Münter, T. L. Andresen, J. B. Larsen, *J. Vis. Exp.* **2019**, e60538.
- [48] C. Lohr, A. H. Kunding, V. K. Bhatia, D. Stamou, in *Methods Enzymol.*, **2009**, pp.

143–160.

- [49] J. C. Stachowiak, F. M. Brodsky, E. A. Miller, *Nat. Cell Biol.* **2013**, *15*, 1019.
- [50] W. F. Zeno, U. Baul, W. T. Snead, A. C. M. DeGroot, L. Wang, E. M. Lafer, D. Thirumalai, J. C. Stachowiak, *Nat. Commun.* **2018**, *9*, 4152.
- [51] T. Ishida, K. Masuda, T. Ichikawa, M. Ichihara, K. Irimura, H. Kiwada, *Int. J. Pharm.* **2003**, *255*, 167.
- [52] N. S. Merle, S. E. Church, V. Fremeaux-Bacchi, L. T. Roumenina, *Front. Immunol.* **2015**, *6*, DOI 10.3389/fimmu.2015.00262.
- [53] F. Chen, G. Wang, J. I. Griffin, B. Brenneman, N. K. Banda, V. M. Holers, D. S. Backos, L. Wu, S. M. Moghimi, D. Simberg, *Nat. Nanotechnol.* **2017**, *12*, 387.
- [54] B. Ashok, L. Arleth, R. P. Hjelm, I. Rubinstein, H. Önyüksel, *J. Pharm. Sci.* **2004**, *93*, 2476.
- [55] A. Nardin, M. Lefebvre, K. Labroquere, O. Faure, J. Abastado, *Curr. Cancer Drug Targets* **2006**, *6*, 123.
- [56] J. E. Frampton, *Pediatr. Drugs* **2010**, *12*, 141.
- [57] S. M. Moghimi, I. Hamad, T. L. Andresen, K. Jørgensen, J. Szebeni, *FASEB J.* **2006**, *20*, 2591.
- [58] M. T. Michalek, E. G. Bremer, C. Mold, *J. Immunol.* **1988**, *140*, 1581 LP.
- [59] B. S. Blaum, J. P. Hannan, A. P. Herbert, D. Kavanagh, D. Uhrin, T. Stehle, *Nat. Chem. Biol.* **2015**, *11*, 77.
- [60] T. M. Allen, A. Chonn, *FEBS Lett.* **1987**, *223*, 42.
- [61] D. C. Litzinger, L. Huang, *Biochim. Biophys. Acta - Biomembr.* **1992**, *1104*, 179.
- [62] D. Liu, A. Mori, L. Huang, *Biochim. Biophys. Acta - Biomembr.* **1992**, *1104*, 95.
- [63] N. S. Merle, R. Noe, L. Halbwachs-Mecarelli, V. Fremeaux-Bacchi, L. T. Roumenina, *Front. Immunol.* **2015**, *6*, DOI 10.3389/fimmu.2015.00257.
- [64] Y.-H. Kim, K. H. Min, Z. Wang, J. Kim, O. Jacobson, P. Huang, G. Zhu, Y. Liu, B.

- Yung, G. Niu, X. Chen, *Theranostics* **2017**, 7, 962.
- [65] S. Ram, A. K. Sharma, S. D. Simpson, S. Gulati, D. P. McQuillen, M. K. Pangburn, P. A. Rice, *J. Exp. Med.* **1998**, 187, 743.
- [66] A. Mori, A. L. Klibanov, V. P. Torchilin, L. Huang, *FEBS Lett.* **1991**, 284, 263.
- [67] Y. S. Park, L. Huang, *Biochim. Biophys. Acta - Lipids Lipid Metab.* **1993**, 1166, 105.
- [68] D. Liu, F. Liu, Y. K. Song, *Pharm. Res.* **1995**, 12, 508.
- [69] D. Liu, Y. K. Song, F. Liu, *Pharm. Res.* **1995**, 12, 1775.
- [70] A. L. Klibanov, K. Maruyama, V. P. Torchilin, L. Huang, *FEBS Lett.* **1990**, 268, 235.
- [71] X. Yan, G. L. Scherphof, J. A. A. M. Kamps, *J. Liposome Res.* **2005**, 15, 109.
- [72] M. Barz, R. Luxenhofer, R. Zentel, M. J. Vicent, *Polym. Chem.* **2011**, 2, 1900.
- [73] K. Kristensen, R. Münter, P. J. Kempen, M. E. Thomsen, A. Stensballe, T. L. Andresen, *Acta Biomater.* **2021**, 130, 460.
- [74] L. Belfiore, L. M. Spenkeliink, M. Ranson, A. M. van Oijen, K. L. Vine, *J. Control. Release* **2018**, 278, 80.
- [75] J. B. Simonsen, E. B. Kromann, *J. Control. Release* **2021**, 335, 660.
- [76] M. Scotuzzi, J. Kuipers, D. I. Wensveen, P. de Boer, K. W. Hagen, J. P. Hoogenboom, B. N. G. Giepmans, *Sci. Rep.* **2017**, 7, 45970.
- [77] J.-M. Rabanel, V. Adibnia, S. F. Tehrani, S. Sanche, P. Hildgen, X. Banquy, C. Ramassamy, *Nanoscale* **2019**, 11, 383.
- [78] J.-B. Coty, C. Vauthier, *J. Control. Release* **2018**, 275, 254.
- [79] V. K. Bhatia, K. L. Madsen, P.-Y. Bolinger, A. Kunding, P. Hedegård, U. Gether, D. Stamou, *EMBO J.* **2009**, 28, 3303.
- [80] M. B. Jensen, V. K. Bhatia, C. C. Jao, J. E. Rasmussen, S. L. Pedersen, K. J. Jensen, R. Langen, D. Stamou, *J. Biol. Chem.* **2011**, 286, 42603.
- [81] A. E. Nel, L. Mädler, D. Velegol, T. Xia, E. M. V. Hoek, P. Somasundaran, F. Klaessig, V. Castranova, M. Thompson, *Nat. Mater.* **2009**, 8, 543.

- [82] S. Schöttler, K. Landfester, V. Mailänder, *Angew. Chemie Int. Ed.* **2016**, *55*, 8806.
- [83] J. Szebeni, L. Baranyi, S. Savay, J. Milosevits, R. Bunger, P. Laverman, J. M. Metselaar, G. Storm, A. Chanan-Khan, L. Liebes, F. M. Muggia, R. Cohen, Y. Barenholz, C. R. Alving, *J. Liposome Res.* **2002**, *12*, 165.
- [84] R. Eliassen, T. Lars Andresen, J. Bruun Larsen, *Eur. J. Pharm. Biopharm.* **2022**, *171*, 80.
- [85] R. Münter, K. Kristensen, D. Pedersbæk, J. B. Larsen, J. B. Simonsen, T. L. Andresen, *Nanoscale* **2018**, *10*, 22720.
- [86] P. M. Bendix, M. S. Pedersen, D. Stamou, *Proc. Natl. Acad. Sci.* **2009**, *106*, 12341.
- [87] J. B. Larsen, C. Kennard, S. L. Pedersen, K. J. Jensen, M. J. Uline, N. S. Hatzakis, D. Stamou, *Biophys. J.* **2017**, DOI 10.1016/j.bpj.2017.06.051.
- [88] E. Elizondo, J. Larsen, N. S. Hatzakis, I. Cabrera, T. Bjørnholm, J. Veciana, D. Stamou, N. Ventosa, *J. Am. Chem. Soc.* **2012**, DOI 10.1021/ja2086678.
- [89] B. Lohse, P.-Y. Bolinger, D. Stamou, *J. Am. Chem. Soc.* **2008**, *130*, 14372.

**Table of Contents entry:**

An imaging assay for studying binding of complement proteins and antibodies to individual liposomes is presented. Association heterogeneities are revealed, as opsonized and non-opsonized liposomes are found to co-exist in the same ensemble. Modification of the liposomal surface with PEG or drugs increases both the percentage of opsonized liposomes and the opsonin surface density on the liposomes.

R. Münter, C. Stavnsbjerg, E. Christensen, M. E. Thomsen, A. Stensballe, A. E. Hansen, L. Parhamifar, K. Kristensen, J. B. Simonsen, J. B. Larsen\*, T. L. Andresen\*

**Unravelling heterogeneities in complement and antibody opsonization of individual liposomes as a function of surface architecture**

